Geoderma 286 (2017) 139–152

Contents lists available at ScienceDirect

Geoderma

journal homepage: www.elsevier.com/locate/geoderma

Salt-affected soils evolution and fluvial dynamics in the Pantanal wetland, Brazil

Sheila Aparecida Correia Furquim [a,*], Marjory Araujo Santos [a], Thiago Tavares Vidoca [a], Marcelo de Almeida Balbino [b], Evaldo Luis Cardoso [c]

[a] Universidade Federal de São Paulo-UNIFESP, Diadema, SP, Brazil
[b] Universidade de São Paulo-USP, São Paulo, SP, Brazil
[c] Empresa Brasileira de Pesquisas Agropecuárias, EMBRAPA, Corumbá, MS, Brazil

ARTICLE INFO

Article history:
Received 30 June 2016
Received in revised form 19 October 2016
Accepted 23 October 2016
Available online xxxx

Keywords:
Solodization
Solonetz
Solodized Solonetz
Solod
Alluvial fan
Intermittent watercourse

ABSTRACT

In the Nhecolândia, a subregion of the Pantanal wetland, saline lakes and their associated Saline-Sodic soils have been degraded due to the atypical input of freshwater from seasonal flooding. In the present work, the soils in and around three brackish lakes that have experienced degradation (Carandazal, Cerca and Banhado lakes) were studied through a detailed morphological survey and chemical analyses to understand their genesis and establish genetic relationship with the Saline-Sodic soils of the saline lakes. The studied soils have Bnc and Bc horizons with morphological and chemical similarities to the Bnx formed around the saline lakes, presenting greenish colors, hard consistencies and, generally, the highest values of pH, exchangeable sodium percentage (ESP), sodium adsorption ratio (SAR) and electrical conductivity in the saturated paste (EC_s) of each profile. In contrast, the near-surface horizons tend to present the lowest values of pH and the highest amounts of Al^{3+} saturation and exchangeable H + Al. These data point to the replacement of salinization/solonization around the saline lakes to the solodization process in the studied soils, with leaching of exchangeable bases, their substitution by Al^{3+} and H^+ and a consequent decrease in pH, first at shallow depths and later in the whole profile. Solodization occurs to a lower degree in the soils associated with the Carandazal lake, which has a predominance of Solonetzes and the closest water pH and electrical conductivity (EC) to the saline lakes, and to a higher degree in the soils related to the Banhado lake, which has a predominance of Solods and the most similar water pH and EC to the freshwaters of the Nhecolândia. The Cerca lake has an intermediate water geochemistry between the studied lakes and an equal prevalence of Solodized Solonetzes and Solods. Soil leaching occurs due to increasing inundation by freshwater through erosion around the saline lakes, primarily involving formation of new intermittent watercourses.

1. Introduction

Salt-affected soils are commonly defined as those containing an excess of soluble salts (Saline, Solonchaks), high amounts of Na^+ in the exchange complex (Sodic, Solonetz, Alkali), or both (Saline-Sodic or Saline-Alkali) (USSL Staff, 1954; Bohn et al., 2001; Sparks, 2003). Their classical model of genesis, initially proposed by Gedroiz (1912, 1917, 1925), is valid in many regions (Kellog, 1934; Kisel, 1981; Zaidel'man et al., 2010; Miller and Brierley, 2011), although different genetic pathways have been observed worldwide (Wilding et al., 1963; Hallsworth and Waring, 1964; Munn and Boehm, 1983; Zaidel'man et al., 2014).

Gedroiz's model and later contributions postulate that Saline, Sodic and a degraded Sodic soil originate in a sequence of soil evolution. In the first stage, Solonchaks (Saline soils) are formed from non-salt-affected soils by a process called salinization, characterized by the accumulation of salts more soluble than gypsum in the soil profile (mainly chlorides and sulfates of sodium, magnesium, calcium and potassium) and a consequent increase in mono- and divalent cations in the exchange complex (Gedroiz, 1912; USSL Staff, 1954; Fanning and Fanning, 1989; Bui et al., 1998).

Solonetzes (Sodic soils) originate in the second stage, deriving from Saline soils by the leaching of most of the soluble salts and/or the precipitation of Ca^{2+} and Mg^{2+} minerals, with a relative increase in exchangeable Na^+ and common occurrence of sodium carbonates (Gedroiz, 1912; Sumner et al., 1998; Sparks, 2003). This process, known as solonization, is generally responsible for an important increase in the soil pH, generally higher than 8.5 (USSL Staff, 1954; Fanning and Fanning, 1989; Schaetzl and Anderson, 2005), mainly because of the liberation of hydroxyls to the solution by both sodium hydrolysis[1] and the dissolution of sodium carbonates[2] (Bohn et al., 2001; McBride, 1994).

* Corresponding author.
E-mail address: sacfurquim@gmail.com (S.A.C. Furquim).

[1] $NaX + H_2O \rightarrow HX + NaOH$, where X is the exchange complex (Bohn et al., 2001).
[2] $Na_2CO_3 \rightarrow 2Na + CO_3^{2-}$; $CO_3^{2-} + H_2O \rightarrow HCO_3^- + OH^-$ (McBride, 1994)

http://dx.doi.org/10.1016/j.geoderma.2016.10.030
0016-7061/

Finally, the continued leaching in the environment leads to a different process called solodization, responsible for the formation of a degraded Sodic soil (Soloth) (Gedroiz, 1925; Kellog, 1934). Solodization is marked by a loss of sodium and other basic cations and an increase of H^+ in the exchange complex, first in the near-surface horizons and later in the whole profile. The soils formed in the initial stages of solodization are conventionally called Solodized Solonetz (Westin, 1953; Janzen and Moss, 1956; Whittig, 1959; Hallsworth and Waring, 1964; Miller and Pawluk, 1994; Anderson, 2010), whereas those formed in the final stages are called Soloth (Kellog, 1934), Solod (Westin, 1953; Heck and Mermut, 1992; Miller and Pawluk, 1994; Zaidel'man et al., 2010) or Solodi (Janzen and Moss, 1956; Whittig, 1959).

Typical Solonetz occurs in regions with: i) evapotranspiration higher than precipitation rates in at least part of the year, allowing for the concentration of soil solutions (Bohn et al., 2001); ii) a temporary availability of humidity, important for the instability of aggregates and subsequent colloid dispersion, especially in the natric horizon (Rengasamy and Sumner, 1998; van Breemen and Buurman, 2003); and iii) low slope gradients associated with near-impervious horizons and/or high water table levels, which restrict subsurface water flows and permit the necessary accumulation of water for high evaporation rates (Westin, 1953; USSL Staff, 1954).

The establishment and evolution of solodization and the consequent genesis of Solodized Solonetz and Solod soils are generally related to a change in one or more of these conditions, triggering an increase in soil leaching. Heck and Mermut (1992), studying salt-affected soils around a saline lake in Saskatchewan (Canada), showed that the formation of terraces due to the lake retreat produced higher topographical levels, promoting lateral leaching conditions and, consequently, the origin of Solodized Solonetzes. Whittig (1959) in California (USA) and Munn and Boehm (1983) in Montana (USA) attributed the genesis of Solodized Solonetzes to a lowering of the water table, enhancing the downward migration of ions. In Montana, specifically, the authors linked this change to a conversion from a post-glacial humid climate to a semi-arid climate 4000 years BP.

The Nhecolândia region (26,921 km^2), located in the central-southern Pantanal wetland (Fig. 1a), has hundreds of saline lakes (*salinas*) surrounded by Saline-Sodic soils (Silva and Abdon, 1998; Furquim et al., 2008; Costa et al., 2015) and thousands of freshwater lakes (*baías*) surrounded by sandy and acid soils not affected by salts (Sakamoto, 1997; Fernandes, 2000; Costa et al., 2015) (Fig. 1b). The saline lakes are on the top of elongated sand hills (*cordilheiras*), which represent the highest topographical level of the region, only 2 to 5 m higher than the surroundings. Typically, the sand hills and, consequently, the saline lakes are not reached by the freshwater that seasonally floods the wetland, allowing for the presence of forested savanna in the sand hills and in the surroundings of the saline lakes, in the outer position of a bare soil ring around the water level (Fig. 1b). In contrast, the freshwater lakes occur in the lowest areas, within long intermittent watercourses (*vazantes*) that seasonally flood, mainly during the summer (Barbiéro et al., 2002). Freshwater lakes and intermittent watercourses are typically occupied by open grass savanna and swampy grasslands (Fernandes, 2000; Evans and Costa, 2013) (Fig. 1b).

However, some lines of evidence suggest that some of the saline lakes have been converted into brackish lakes by atypical input of freshwater within the sand hills, creating new intermittent watercourses. First, the dense forested savanna that usually covers the sand hills fully surrounds the saline lakes but occurs only partially around the brackish lakes. The presence of non-forested zones and the disappearance of the bare soil ring around the saline lakes, both usually replaced by open woody savanna and grasslands, point to a partial degradation of the slightly higher and fragile sand hills, which would allow for intermittent flooding (Fernandes, 2007; Almeida et al., 2003; Evans and Costa, 2013). Second, the association of degraded natric horizons with some brackish lakes, similar to those typically created in the geochemical conditions of saline lakes, suggests a genetic relationship between them (Rezende Filho, 2006; Barbiero et al., 2008).

The destruction of the saline lakes and their replacement by brackish lakes would provoke intense transformation in the Saline-Sodic soils, especially through leaching related to the advancement of the freshwater from seasonal flooding. Although the salt-affected soils occurring around the saline lakes have been extensively studied (Furquim et al., 2008; Furquim et al., 2010a; Furquim et al., 2010b; Martins, 2012), those associated with the brackish lakes are known mainly by morphological descriptions, accompanied by a few laboratory analyses (Rezende Filho, 2006; Silva, 2007).

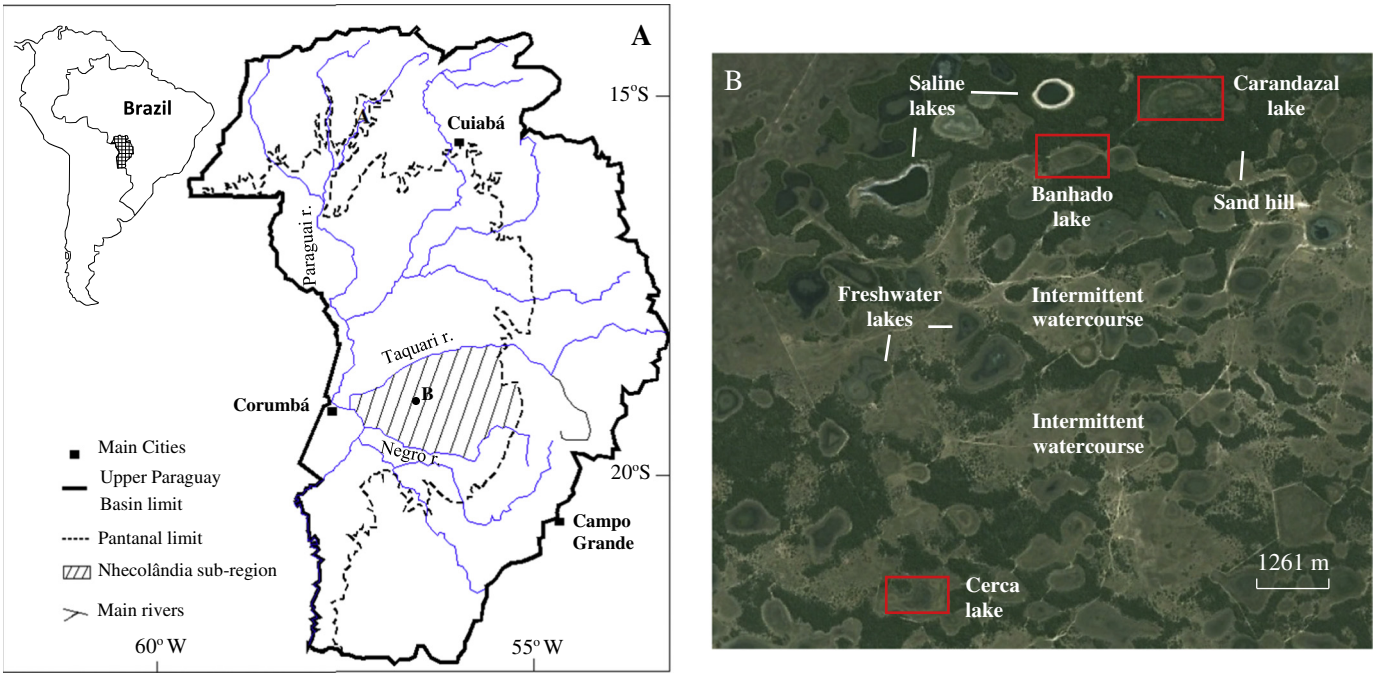

Fig. 1. A) Pantanal wetland and Nhecolândia subregion; B) Nhumirim farm: examples of the main geomorphological elements of the low Nhecolândia (sand hills, saline lakes, freshwater lakes, intermittent watercourses) and location of the studied brackish lakes (Carandazal, Cerca and Banhado).

In this context, the present work aimed to better investigate the characteristics and origin of the soils associated with representative brackish lakes, assuming that freshwater entrance in the saline lakes could be responsible for transformation of their Saline-Sodic soils, generating degraded Sodic soils such as Solodized Solonetzes and Solods. In contrast to what has been reported in the literature, the leaching responsible for the genesis of these soils would be directly related to the current fluvial dynamics, with the origin of new intermittent watercourses and freshwater lakes.

2. Materials and methods

2.1. Environmental setting

The Pantanal wetland, located in the Upper Paraguay drainage basin, is one of the largest wetlands of the world (150,500 km^2), with 90% of its area in Brazil and 10% in Bolivia and Paraguay (16°–20° S; 50°–58° W) (Padovani, 2010; Assine, 2015) (Fig. 1a). Although deforestation has intensified in the last decades (Silva et al., 2011; Bacani et al., 2016), the region still has well-preserved ecosystems, with a low population density and economic activity mainly based on extensive animal husbandry (Por, 1995; Assine, 2015; Pott and Silva, 2016). The Pantanal biome presents large aquatic and terrestrial biodiversity and is characterized by the convergence of the Cerrado (Brazilian savanna), the Amazon, the Atlantic Forest and the Chaco biogeographical provinces (Adámoli, 1986; Silva et al., 2001; Pott and Silva, 2016). Because of its environmental qualities, it is considered a wetland of international importance by the Ramsar Convention of Wetlands and part of its area is recognized as a World Heritage Area by UNESCO.

According to Koppen's classification, the climate of the Pantanal is Tropical Savanna-Aw (Por, 1995), characterized by mean annual temperatures between 22.4° and 25.6° C (Tarifa, 1986) and mean annual precipitation from 850 to 1100 mm, with marked wet (December to March) and dry (June to August) periods (Alvarenga et al., 1984; Alfonsi and Camargo, 1986). Although seasonally there is a high availability of water, the annual potential evapotranspiration of at least 1400 mm impresses an annual hydric deficit higher than 300 mm in the wetland (Alfonsi and Camargo, 1986).

The whole wetland is an active sedimentary basin filled with sandy, silt-sandy and clayey unconsolidated or semi-consolidated materials that have been deposited along the Cenozoic, reaching a sedimentary thickness up to 500 m in the center of the depression (Del'Arco et al., 1982; Godoi Filho, 1986; Assine et al., 2005; Assine, 2015). Alluvial fans are the most common depositional system, but floodplains and lacustrine systems are also commonly found in the basin (Assine, 2003; Assine et al., 2015). The region presents altitudes between 80 and 200 m and extremely low slope gradients (0.02 to 0.03°), being partially covered by seasonal inundation (Assine, 2015; Silva, 1986; Scott, 1991). Most of the flooding water and the deposited sediments come from surrounded highlands (200 to 900 m), which are formed by Precambrian crystalline and Mesozoic sedimentary rocks (Del'Arco et al., 1982; Alvarenga et al., 1984; Godoi Filho, 1986; Por, 1995).

The flooding in the Pantanal starts 2 to 3 months from the beginning of the wet season (Padovani, 2010) with the inundation pulse reaching its maximum during the dry season (June to July) in the southernmost subregions (Carvalho, 1986; Hamilton et al., 1996). The flooding may occur due to an overbank flow of the main rivers, the upstream restriction of tributary drainage due to inundation of the Paraguay River, or an accumulation of local rainfall water, with the last of which being the largest source of water to the Nhecolândia (Hamilton, 1999). The peak of the inundation in the low Nhecolândia (area of 8220 km^2), where the association between freshwater, brackish and saline lakes occurs, may vary from February to May, depending on the year, with a monthly average flooding area during this period near 4000 km^2 (Hamilton et al., 1996; Costa et al., 2015). The saline lakes do not typically dry out during the year and, in general, are not reached by surface waters during flooding as they are fed mainly by ground water and rainfall. In contrast, freshwater and brackish lakebeds, which are reached by seasonal inundation, are usually free of surface water during the peak of the dry period (Silva, 2007; Rezende Filho, 2006).

The waters associated with freshwater lakes and intermittent watercourses present pH values between 4.6 and 7.9 and electrical conductivity (EC) between 0.01 and 0.30 dS m^{-1}. In contrast, the surface and subsurface waters related to the saline lakes have much higher pH and EC values, respectively varying from 8.5 to 10.1 and 6 to 68 dS m^{-1} (Barbiéro et al., 2002; Almeida et al., 2003; Parizotto, 2012). In spite of this huge geochemical variability, even in short distances (≥200 m), all the waters of the low Nhecolândia belong to the same chemical family, which is evolving through evaporative concentration as a result of the high evapotranspiration rates of the wetland (Barbiéro et al., 2002; Almeida et al., 2010). The saline lakes experience a higher concentration because of their isolation within the sand hills, which prevents the seasonal input of freshwater by flooding (Barbiero et al., 2008).

This variability in water conditions triggers significant morphological, chemical and physical differences in the soils. Sand hills, intermittent watercourses and freshwater lakes are dominated by Psamments (A over C horizons), with ≤50 g kg^{-1} of clay, no structure (single grain) and an acidic pH (generally ≤5). Sand hills also have Spodosols, with a sequence of A - Bh (or Bs) - C horizons, characterized by a sandy texture (>850 g kg^{-1} of sand) and acid to neutral pH (5 to 7) (Cunha, 1980; Queiroz Neto et al., 1997; Sakamoto, 1997; Silva and Sakamoto, 2003; Fernandes, 2000).

Around the saline lakes, the Saline-Sodic soils have, in general, a pale brown, fine sand and single grain surface horizon, which can be laterally replaced, in the area of seasonal lake-level variation, by a dark gray, loamy sand and prismatic H horizon. Below these bare surface horizons commonly occurs a light brownish gray, fine sand and single grain E horizon, which may have vertical mottles enriched in organic matter. This horizon overlies a gray, loamy sand and massive Bkg, with abundant carbonate nodules (calcite, dolomite and/or nahcolite). Finally, the deepest horizon is generally an extremely hard and poorly permeable Bnx, marked by an olive color, sandy loam texture and lack of structure (massive) (Sakamoto, 1997; Barbiéro et al., 2000; Silva and Sakamoto, 2003; Silva et al., 2004; Furquim, 2007).

Detailed research performed by Furquim (2007), Furquim et al. (2010a) and Martins (2012) showed that most of the soils around the saline lakes present exchangeable sodium percentage (ESP) higher than 30%, electrical conductivity (EC$_s$) higher than 10 dS m^{-1}, pH in general higher than 9 but commonly 10 or more, and very low or an absence of exchangeable Al^{3+} or H + Al. Although salinization is apparently present, these soils seem to be mainly governed by solonization, with an important presence of Na^+ in the exchange complex and consequent alkalization, leading to an extremely alkaline pH. The relative gathering of exchangeable sodium is improved by the involvement of Ca^{2+} and Mg^{2+} in the direct precipitation of carbonates (calcite and dolomite) and magnesian smectites (stevensite and saponite) (Furquim et al., 2008; Furquim et al., 2010a).

Soil surveys based on morphological data, field electromagnetic conductivity (EC$_e$) and pH measurements in and around two brackish lakes, one more mineralized (pH and EC close to saline lakes) and the other less mineralized (pH and EC close to freshwaters), show a similar soil organization to the Saline-Sodic soils (Silva, 2007; Rezende Filho, 2006). Horizons similar to the gray Bkg and the olive Bnx are present in and around both of the lakes, but in and around the less mineralized, these horizons occur in a discontinuous form. These soils are, however, different from the saline lake, mainly in terms of having lower EC$_e$, reaching 80 and 100 dS m^{-1} in the soils of the less and more mineralized lake, respectively, in contrast to 400 dS m^{-1} in the Saline-Sodic soils (Silva, 2007; Rezende Filho, 2006; Barbiero et al., 2008). Silva (2007) also reported lower pH in the soils of the more mineralized brackish lake than in the soils of the saline lakes, with values ranging,

in the former, from 7.0 to 7.9 near the surface and from 8.0 to 8.9 in the B horizons.

2.2. Methods

The research was conducted in and around three ephemeral brackish lakes with intermediate geochemistry characteristics between fresh and saline waters: Carandazal (pH: 6.54; EC: 1.88 $dS \cdot m^{-1}$), Cerca (pH: 6.40; EC: 1.10 $dS\ m^{-1}$) and Banhado (pH 6.17; CE: 0.76 $dS\ m^{-1}$) (Almeida et al., 2003). They are all located in the low Nhecolândia, Mato Grosso do Sul state, specifically at the Nhumirim Farm, property of EMBRAPA, the Brazilian Agricultural Research Corporation (Fig. 1b). Field work was carried out over three consecutive years, always during the dry season, when the lakes were dry.

The soil survey was performed along three transects (T), one associated with each lake (T1-Carandazal, T2-Cerca and T3-Banhado), according to the methodology of Structural Analysis of the Pedological Cover, which is the study of the morphological characteristics, the lateral/vertical distribution and the geometrical arrangement of soils (horizons, structures, constituents) along geomorphological units (Boulet, 1992; Ruellan and Dosso, 1993). In and around the Carandazal and Cerca lakes, the transects (T1 and T2) start at the border of the sand hill and end at the lowest point of the lake depression, whereas in and around the Banhado lake, the transect (T3) extends between two borders of the sand hill, intersecting the center of the dry lake (Fig. 2).

Each transect's topography was obtained by direct differential leveling between two points of a sequence. The distance and the elevation difference between two points were determined, respectively, by a 30 m tape line and by a flexible, transparent and water-filled tube between them. The relative height of the two points was obtained by measuring, with a 1 m scale, the water level at the extremities of the tube (Torge and Muller, 2012). Soil morphology descriptions were carried out according to Schoeneberger et al. (2002) on a total of thirty auger holes, which allowed us to preliminarily organize the horizons in the transects, and twelve trenches, located in representative zones or in lateral transitions between horizons.

Samples of all the identified horizons were taken mainly from the trenches, air-dried, sieved to produce the fine earth fraction (<2 mm), quartered by the elongated pile method (Góes et al., 2004) and submitted to laboratory analyses. The 1:1 soil-water, 2:1 soil-$CaCl_2$ and 1:1 soil-KCl pH were measured according to USDA (2014). Exchangeable Ca^{2+}, Mg^{2+} and Al^{3+} were extracted by the addition of 1 M KCl, with Ca^{2+} and Mg^{2+} determined by atomic absorption spectroscopy (AAS) and Al^{3+} by titration with 0.025 M NaOH, using bromothymol blue as the indicator (Cantarella et al., 2001). Exchangeable Na^{+} and K^{+} were extracted with a Mehlich 1 solution (0.05 M HCl + 0.0125 M H_2SO_4) and measured by flame photometry (Silva et al., 2009). H + Al were extracted with 0.5 M $(CH_3COO)_2Ca \cdot H_2O$ at pH 7 and quantified by titration with 0.025 M NaOH, using the indicator phenolphthalein (Quaggio and Raij, 2001). The cation exchange capacity (CEC) was calculated as the sum of the bases (Ca^{2+}, Mg^{2+}, Na^{+} and K^{+}) and H + Al (EMBRAPA, 1997). These analyses were performed in triplicate, accepting a coefficient of variation (CV) of ≤12%.

The saturated paste of each sample was prepared by adding deionized water to 150–500 g of the quartered fine-earth fraction, until the criteria adopted by USDA (2014) were achieved (glistening, slight flowing with movement and free sliding from a spatula). The paste was permitted to stand overnight and the extract was obtained with the assistance of a vacuum system to measure pH_s, electrical conductivity (EC_s) and the main cations in the solution. Na^{+} and K^{+} were determined by flame photometry and Ca^{+2} and Mg^{+2} by atomic absorption spectroscopy (AAS). Then, the sodium adsorption ratio (SAR) was calculated according to the following formula: $Na/[(Ca + Mg)/2]^{1/2}$, using soluble Na^{+}, Ca^{2+} and Mg^{2+} concentrations in $mmol_c\ L^{-1}$ (Bohn et al., 2001; Sumner et al., 1998).

3. Results

3.1. Soil morphology

The soil organization along the three transects (T1-Carandazal, T2-Cerca, T3-Banhado) and the morphological data are shown in Fig. 3. Seventeen horizons were recognized, five occurring in all the transects (A1, A2, Bw1, Bnc1, Bnc2), four appearing at T2 and T3 (Bw4, Bg1, AC, C1), one appearing at T1 and T3 (AB) and the others with a local distribution

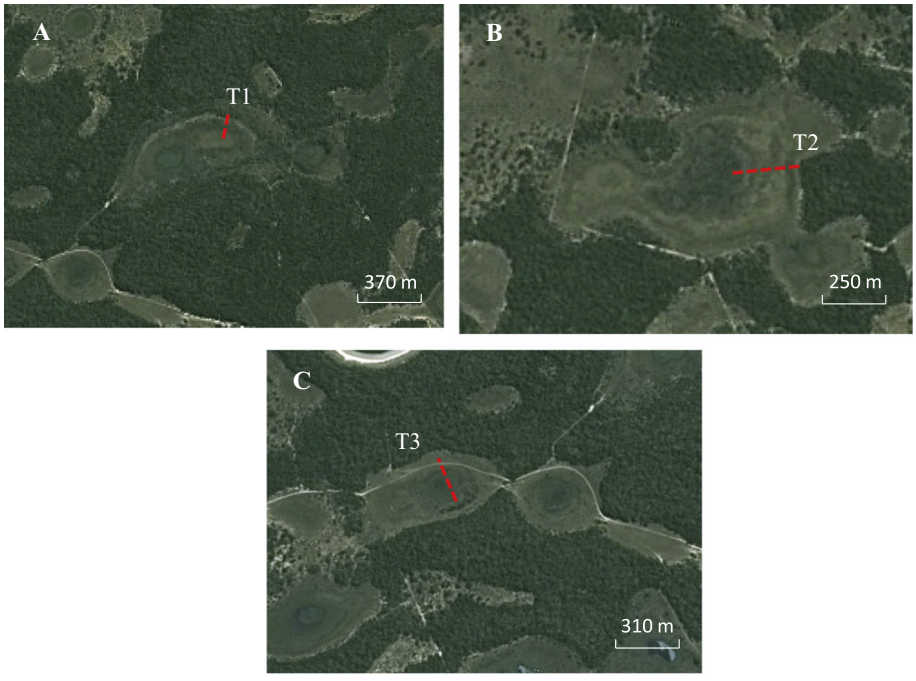

Fig. 2. Soil survey in transects (dashed lines) at: A) Carandazal lake (T1-Transect 1); B) Cerca lake (T2-Transect 2); and C) Banhado lake (T3-Transect 3). Images source: Google™ Earth (2016).

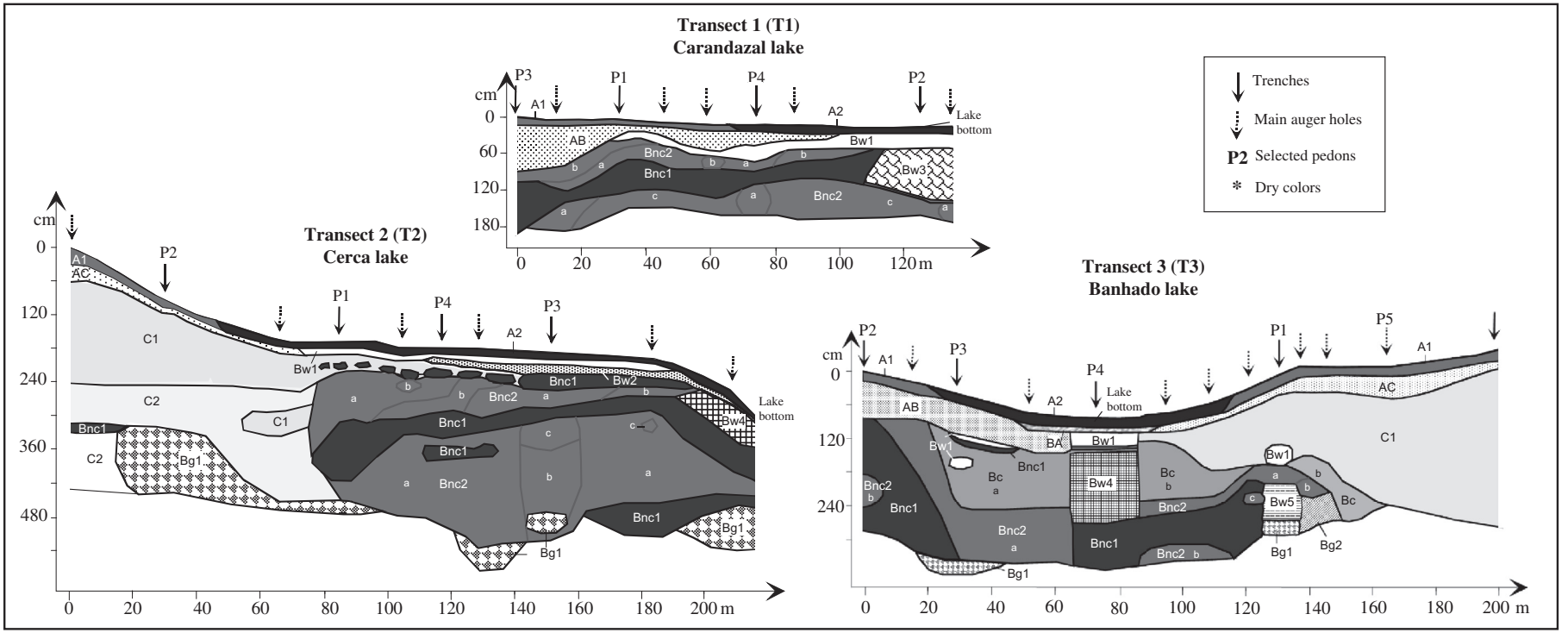

A1: Dark grayish brown* (10YR 4/2); fine sand; granular or subangular blocks, weak to moderate; low excavation difficulty.

A2: Very dark grayish brown* (10YR 3/2) or dark gray* (10YR 4/1); fine sandy loam to silt loam; platy or subangular blocks; moderate; low excavation difficulty.

AB: Brown* (10YR 5/3) or pale brown* (10YR 6/3); fine sand; single grain; low excavation difficulty.

BA: Gray* (10YR 6/1); loamy fine sand; massive; very high excavation difficulty. Yellowish brown (10YR 5/6) redox features.

Bw1: Light gray* (10YR 7/1, 6/2); fine sandy loam; massive; very high excavation difficulty. It presents strong brown (7.5YR 4/6, 5/8, 5/6) or reddish yellow (7.5YR 6/8) redox features.

Bw2: Light brownish gray* (2.5Y 6/2); fine sand; massive; moderate excavation difficulty.

Bw3: Intermingled: gray* (10YR 6/1), grayish brown* (2.5Y 5/2) and olive* (5Y 5/3); sandy clay loam; massive; very high excavation difficulty. It presents features i and iii described in horizon Bnc 1, Bnc2 and Bc, but in less amounts.

Bw4: Very dark grayish brown* (2.5Y 3/2); loam; massive; very high excavation difficulty. It presents features I and iv described in horizon Bnc1, Bnc2 and Bc, but in less amounts.

Bw5: Yellowish brown* (10YR 5/6) or red (2.5YR 5/6); sandy clay loam; massive; moderate excavation difficulty. Strong brown (7.5YR 5/8) redox features.

Bnc1: Olive* (5Y 4/4, 4/3); fine sandy loam to sandy clay loam; massive or weak subangular blocky structure; very high excavation difficulty. Presence of one or more of the following features: i) black* (Gley 1 N 2.5/), very hard nodules, with metallic lustre; ii) black* (10YR 2/1, 2.5Y 2.5/1) and clayey mottles; iii) white* (White Page, N 9.5/), very hard nodules, with no HCl reaction; iv) dark yellowish brown* (10YR 4/6) or strong brown* (7.5YR 4/6) redox features; v) nodules similar to horizon Bnc2 in color and texture.

Bnc2: Greenish (2.5Y hue), with the following colors: a-olive brown* (4/3, 4/4), b-dark grayish brown* (4/2), c-light olive brown* (5/4); fine sandy loam to sandy clay loam; massive or weak subangular blocky structure; very high excavation difficulty. It presents at least one of the features i to iv described in horizon Bnc1 and nodules similar to horizon Bnc1 in color and texture.

Bc: matrix 10YR, with the following colors: a-dark yellowish brown* (4/4), b-brown* (4/3 or 5/3); fine sandy loam to clay loam; massive or weak subangular blocky structure; high excavation difficulty. It presents at least one of the features i to iv described in horizon Bnc1 and Bnc2.

Bg1: Greenish gray* (Gley 1, 10Y 5/1); fine sand, loamy fine sand or fine sandy loam; massive; moderate excavation difficulty. Dark greenish gray* (Gley 1, 10 GY 4/1) mottles and nodules.

Bg2: Very dark gray* (Gley 1, N 3/); fine sand to loamy fine sand; massive; moderate excavation difficulty. Olive* (5Y 5/6, 4/4) mottles or nodules.

AC: Brown* (10YR 5/3); fine sand; single grain; low excavation difficulty.

C1: light gray* (10YR 7/2); fine sand; single grain; low excavation difficulty.

C2: Brown* (10YR 4/3); fine sand; single grain; low excavation difficulty.

Fig. 3. Soil organization along the three studied transects.

Table 1
Main chemical properties of selected samples.

Horizons	Depth cm	pH-H_2O	pH-$CaCl_2$	pH-KCl	Al^{3+}	H + Al	Ca^{2+}	Mg^{2+}	K^+	Na^+	CEC	Base sat.	Al^{3+} sat.	ESP
					$mmol_c\ kg^{-1}$							%		
Transect 1 (T1) – Carandazal lake														
Pedon 3 (P3)														
A1	0–16	6.71	6.06	6.30	0.00	6.27	41.60	10.53	10.78	6.01	75.2	91.7	0.0	8.0
AB	16–90	6.81	6.13	6.29	0.00	2.33	2.79	0.00	3.94	5.25	14.3	83.7	0.0	36.7
Bnc2	90–107	9.02	7.71	7.61	0.00	0.60	14.40	3.48	42.05	69.71	130.2	99.5	0.0	53.5
Bnc1	107–192+	8.85	7.71	7.43	0.00	0.00	21.38	7.82	15.30	25.21	69.7	100.0	0.0	36.2
Pedon 1 (P1)														
A1	0–8	6.34	5.77	6.06	0.00	9.20	40.30	9.09	3.34	0.45	62.4	85.3	0.0	0.7
Bw1	18–31	6.88	6.04	6.31	0.00	2.40	5.42	0.95	0.74	0.29	9.8	75.5	0.0	3.0
Bnc2	43–68	8.20	7.35	7.29	0.00	1.47	31.50	7.58	14.88	13.90	69.3	97.9	0.0	20.0
Bnc1	68–118	8.27	7.47	7.08	0.00	2.00	42.01	14.58	23.56	41.81	124.0	98.4	0.0	33.7
Bnc2	118–145+	8.37	7.50	6.86	0.00	2.67	27.52	10.53	17.09	25.30	83.1	96.8	0.0	30.4
Pedon 4 (P4)														
A2	0–9	5.59	4.60	4.91	0.40	52.60	89.67	14.99	6.05	0.52	163.8	67.9	0.4	0.3
AB	9–34	6.27	5.84	6.23	0.00	4.47	4.42	0.53	0.65	0.33	10.4	57.0	0.0	3.2
Bw1	34–60	6.38	6.27	6.40	0.00	2.53	6.64	2.15	1.00	0.31	12.6	80.0	0.0	2.5
Bnc2	60–77	8.38	7.56	7.32	0.00	1.87	45.90	11.41	14.75	13.57	87.5	97.9	0.0	15.5
Bnc1	77–98	8.58	7.37	7.10	0.00	2.47	43.65	13.72	17.81	25.80	103.5	97.6	0.0	24.9
Bnc2	98–132+	8.14	7.07	6.58	0.00	4.00	42.64	18.47	20.95	25.71	111.8	96.4	0.0	23.0
Pedon 2 (P2)														
A2	0–19	5.76	5.09	5.35	0.40	49.60	148.27	35.06	18.72	0.49	252.1	80.3	0.2	0.2
Bw1	19–50	6.77	6.12	6.18	0.00	4.07	8.19	2.49	1.11	0.28	16.1	74.8	0.0	1.7
Bw3	50–122	8.09	7.17	6.80	0.00	3.60	67.72	9.66	14.89	8.80	104.7	96.6	0.0	8.4
Bnc2	122–145+	8.05	6.95	6.19	0.00	1.73	32.17	8.61	15.03	8.79	66.3	97.4	0.0	13.3
Transect 2 (T2) – Cerca lake														
Pedon 2 (P2)														
A1	0–15	5.81	5.48	5.36	0.10	9.60	13.13	1.24	0.98	0.55	25.5	62.4	0.6	2.2
C1	22–145	4.95	4.34	4.13	0.40	3.20	1.22	1.53	0.69	0.43	7.1	54.7	9.4	6.1
C2	145–218	4.88	3.86	3.71	3.00	3.20	1.85	1.28	1.68	0.70	8.7	63.3	35.3	8.0
Bg1	218–331+	5.98	5.44	3.31	3.50	4.20	2.03	1.29	1.60	0.50	9.6	56.3	39.2	5.2
Pedon 1 (P1)														
A2	0–10	5.71	4.87	5.00	0.10	50.27	3.86	3.78	10.45	0.80	69.2	27.3	0.5	1.2
Bw1	10–19	5.54	4.88	4.37	0.20	24.60	40.95	2.74	5.02	0.54	73.9	66.7	0.4	0.7
Bnc1	35–50	6.15	5.37	5.13	0.10	13.60	42.68	3.45	6.33	3.13	69.2	80.3	0.2	4.5
Bnc2	109–125	7.62	6.44	6.19	0.10	2.53	13.12	0.50	3.00	1.90	21.1	88.0	0.5	9.0
Bnc1	138–244	6.75	5.95	5.37	0.10	1.47	34.01	0.13	12.77	2.96	51.3	97.1	0.2	5.8
Bnc2	244–283	6.48	5.55	4.64	0.50	1.93	34.13	2.53	7.00	1.61	47.2	95.9	1.1	3.4
Bg1	283–305+	6.00	5.20	4.85	0.40	2.07	25.52	5.07	3.75	1.18	37.6	94.5	1.1	3.1
Pedon 4 (P4)														
A2	0–10	6.35	5.64	5.62	0.30	33.40	4.29	4.16	7.65	0.85	50.4	33.7	1.7	1.7
Bw1	10–19	6.13	5.34	5.25	0.10	20.73	3.37	3.18	4.77	0.80	32.9	36.9	0.8	2.4
Bw2	19–28	7.16	6.55	6.50	0.10	0.60	11.45	0.95	2.40	0.53	15.9	96.2	0.7	3.3
Bnc1	40–54	7.85	7.09	7.24	0.10	0.00	23.08	0.77	4.57	1.06	29.5	100.0	0.3	3.6
Bnc2	88–110	8.18	7.33	7.18	0.00	0.20	29.18	5.00	8.24	4.44	47.1	99.6	0.0	9.4
Bnc1	110–125	8.20	7.35	7.04	0.00	0.20	25.02	4.57	9.04	4.43	43.3	99.5	0.0	10.2
Bnc2	160–278+	8.12	7.53	7.15	0.00	0.20	22.80	2.53	9.41	4.67	39.6	99.5	0.0	11.8
Pedon 3 (P3)														
A2	0–9	5.59	5.01	5.26	0.50	52.67	4.02	4.93	12.50	0.70	74.8	29.6	2.2	0.9
Bw1	9–20	5.04	4.13	4.40	0.50	25.87	21.07	1.07	3.29	0.57	51.9	50.1	1.9	1.1
Bw2	20–37	6.34	5.46	5.22	0.00	3.00	6.88	1.03	1.57	0.43	12.9	76.8	0.0	3.3
Bnc1	40–65	6.69	5.96	5.38	0.00	2.33	2.47	3.87	7.94	2.33	18.9	87.7	0.0	12.3
Bnc2	65–100	7.83	7.07	6.78	0.00	1.20	41.22	3.47	7.16	3.37	56.4	97.9	0.0	6.0
Bnc1	100–114	8.15	7.38	7.15	0.60	0.40	2.65	5.10	8.52	5.81	22.5	98.2	2.7	25.9
Bnc2	114–170	8.04	7.28	7.04	0.70	0.20	2.61	1.54	10.78	8.26	23.4	99.1	2.9	35.3
Transect 3 (T3) – Banhado lake														
Pedon 2 (P2)														
A1	0–16	5.04	4.50	4.86	0.40	7.20	4.24	0.42	0.47	0.37	12.7	43.3	6.8	2.9
AB	16–82	5.06	5.08	5.28	0.40	0.80	1.00	0.08	0.43	0.25	2.6	68.9	18.5	9.7
Bnc1	82–180	8.70	7.32	7.13	0.00	0.00	26.88	8.16	14.86	25.76	75.7	100.0	0.0	34.0
Bnc2	180–240	8.96	7.57	7.68	0.00	0.00	27.50	11.96	14.67	14.65	68.8	100.0	0.0	21.3
Bnc1	240–280+	8.87	7.45	7.67	0.00	0.00	26.09	13.39	14.88	14.85	69.2	100.0	0.0	21.5
Pedon 3 (P3)														
A2	0–13	5.19	4.40	4.89	0.40	30.40	23.92	7.81	2.35	0.39	64.9	53.1	1.2	0.6
AB	13–71	5.02	4.73	4.84	0.40	1.60	0.60	0.34	0.58	0.52	3.6	56.0	16.4	14.4
Bc	88–115	5.42	4.66	4.36	0.40	25.60	59.55	54.74	5.38	10.18	155.5	83.5	0.3	6.6
Bw1	115–130	5.59	4.84	4.36	0.00	5.60	30.42	25.44	3.47	3.75	68.7	91.9	0.0	5.5
Bc	130–185	6.10	5.43	5.07	0.00	3.20	32.52	12.69	4.40	2.93	55.7	94.3	0.0	5.3
Bnc2	185–291	7.70	6.97	6.70	0.00	0.00	34.99	24.22	2.16	1.48	62.9	100.0	0.0	2.4
Bg1	291–324+	8.04	7.34	7.32	0.00	0.00	23.31	8.92	2.97	2.12	37.3	100.0	0.0	5.7
Pedon 4 (P4)														
A2	0–15	4.92	4.19	4.59	1.60	93.60	51.26	23.50	9.16	0.84	178.4	47.5	1.9	0.5
Bw1	24–50	5.82	5.12	5.30	0.00	0.80	10.22	4.60	2.15	0.49	18.3	95.6	0.0	2.7
Bc	55–61	5.02	4.25	4.41	0.40	23.20	51.72	32.69	0.91	0.37	108.9	78.7	0.5	0.3

Table 1 (*continued*)

Horizons	Depth cm	pH-H_2O	pH-$CaCl_2$	pH-KCl	Al^{3+}	H + Al	Ca^{2+}	Mg^{2+}	K^+	Na^+	CEC	Base sat.	Al^{3+} sat.	ESP
					$mmol_c\ kg^{-1}$							%		
Bw4	61–185	5.77	5.11	5.03	0.40	12.80	40.17	31.46	5.10	2.32	91.9	86.1	0.5	2.5
Bnc1	185–251+	6.72	6.14	5.94	0.00	0.80	12.37	8.48	3.87	1.38	26.9	97.0	0.0	5.2
Pedon 1 (P1)														
A1	0–20	4.60	4.01	4.51	0.80	9.60	5.32	1.50	0.98	0.47	17.9	46.3	8.8	2.6
C1	32–124	5.62	5.52	5.73	0.00	1.60	0.42	0.43	0.33	0.44	3.2	50.2	0.0	13.6
Bw1	124–155	5.15	4.23	4.34	0.40	0.80	4.30	1.63	0.88	1.20	8.8	90.9	4.8	13.6
Bnc2	155–189	5.07	3.86	3.69	1.20	7.20	8.64	7.11	1.67	2.94	27.6	73.9	5.6	10.7
Bw5	189–255	5.28	4.69	4.23	0.80	13.60	32.95	38.30	7.93	5.37	98.2	86.1	0.9	5.5
Bg1	255–275+	6.13	5.34	5.04	0.40	4.80	29.10	35.20	6.98	2.79	78.9	93.9	0.5	3.5
Pedon 5 (S5)														
A1	0–22	5.24	4.31	4.72	0.40	8.80	4.59	1.25	0.53	0.59	15.8	44.2	5.4	3.7
C1	34–232	6.07	5.42	5.47	0.00	1.60	0.78	0.41	0.36	0.59	3.7	57.2	0.0	15.8
C1	232–314+	4.96	4.64	4.43	0.40	0.80	1.58	0.84	0.43	0.60	4.3	81.2	10.4	14.1

at one of the transects (Bw3 at T1; Bw2 and C2 at T2; BA, Bc, Bw5 and Bg2 at T3).

A1, AB, AC, C1 and C2 are fine sand horizons that occur mainly in higher positions, forming thick profile sequences at T2 (e.g., A1-AC-C1-C2) and T3 (e.g., A1-AC-E). A1 has a dark grayish brown color and a mainly granular structure, whereas AB, AC, C1 and C2 are single-grain, having lighter colors in the first three and slightly darker color in the last. Horizons A2, Bw1 and Bw2 occur mainly in lower topography, at or near the surface. A2 is darker than A1 and has a platy and/or subangular block structure. Horizons Bw1 and Bw2 are similar in silt enrichment and lack of structure (massive), but the former is whitish (10YR 7/1, 6/2) and extremely hard whereas the latter is light greenish (2.5Y 6/2) and moderately hard.

The distribution of the Bnc and Bc horizons is variable. Bnc1 and Bnc2 occur in high vertical and lateral continuity along T1 and in intermediate lateral continuity and vertical discontinuity at the low positions of T2. At T3, Bnc1, Bnc2 and Bc have vertical and lateral discontinuity at both high and low positions. A clear morphological resemblance is observed between these three horizons, being all mostly massive, more clayey than the upper horizons and heterogeneous, with volumes of different characteristics distributed in the matrix. A range of matrix color and hardness is observed, being extremely hard and greenish (5Y 4/4, 4/3) at Bnc1, hard to extremely hard and less pronounced green (e.g. 2.5Y 4/4, 4/3) at Bnc2 and hard and brownish (10YR 4/4, 4/3) at Bc. However, the main volumes occurring in the three horizons are similar: i) black nodules, extremely hard, with a metallic luster, abundant at T1 and progressively less so at T2 and T3; ii) black, not cemented but commonly associated with the metallic black nodules, clayey to very clayey and abundant in all the transects; iii) strong brown and yellowish red redoximorphic features, common to rare in the three transects; and iv) volumes similar to the matrix of Bnc1 (5Y 4/4, 4/3) in the Bnc2 (2.5Y 4/4, 4/3) and vice versa, common to rare in the three transects.

The other horizons generally have small and discontinuous distributions and most of them are associated with long groundwater saturation. Horizons Bg1 and Bg2 are relatively deep in the profiles, have fine sandy to fine sandy loam textures and exhibit typical hydromorphic colors in the matrix, such as greenish gray (Gley 1, 10Y 5/1), very dark gray (Gley 1, 3/N) and dark greenish gray (Gley 1, 5GY 4/1, 10Y 4/1). Horizons BA, Bw3 and Bw4 are in the center of the depression and are probably related to the sedimentation dynamics of the lakes. They have a more clayey texture than the contiguous upslope horizons (AB for BA; Bnc1 for Bw3; Bnc1, Bnc2 and Bc for Bw4) and redoximorphic features. Horizons Bw3 and Bw4 also have the same volumes found in the Bnc and Bc horizons, such as the black nodules and greenish (5Y and 2.5Y) masses.

3.2. Chemical analyses

The pH-H_2O varies widely, changing from moderately acid (5.6) to strongly alkaline (9.0) in the Carandazal transect (T1), very strongly acid (4.9) to moderately alkaline (8.2) in the Cerca transect (T2) and very strongly acid (4.6) to strongly alkaline (9.0) in the Banhado transect (T3) (Table 1; Fig. 4). Thus, a general decreasing of pH is observed between the transects, with values smaller than 6.0 occurring in 11% of the samples at T1, 30% at T2 and 65% at T3. In addition, an increase in the values toward greater depths is evident, occurring in most of the pedons from the surface or relatively near-surface horizons (A1, A2, AB, Bw1, Bw2) to the deep subsurface horizons (Bnc1, Bnc2, Bg1). This vertical pattern of distribution, however, is barely or not observed in the sandy zones located in higher topographical positions of T2 (P2) and T3 (P5), where the horizons tend to be acid. Laterally, the pH tends to decrease toward the center of the lake depression at T1 and T3 (especially from P2 to P4), in a subtle way in the former and more clearly in the latter, but generally increases downslope along T2.

Both pH-$CaCl_2$ and pH-KCl are mostly less than pH-H_2O, but the values of these parameters in the same sample are generally similar to each other, varying from 4.6 to 7.7 along T1, 3.3 to 7.5 along T2 and 3.7 to 7.7 along T3 (Table 1). In contrast, the pH values measured in the extract of the saturated paste (pH_s) are higher than pH-H_2O, with values between 6.8 and 9.0 at T1, 5.1 and 8.7 at T2 and 5.1 and 8.8 at T3 (Table 2). However, these three parameters tend to have a similar behavior to pH-H_2O in the three transects, presenting a general decreasing of values from the Carandazal transect (T1) to the Banhado transect (T3) and an increasing of values from shallow to deep horizons of each pedon, with the exception of the sandy zones of T2 (P2) and T3 (P5). Laterally, toward the bottom of the lake, values also tend to decrease along T1 and T3 and increase along T2.

EC_s varies between 0.0 and 8.4 dS m^{-1} along T1, with four values higher than 4 dS m^{-1}, located in horizons Bnc1 and Bnc2 at the middle of the transect (P1, P4) (Table 2, Fig. 4). The values in the Cerca and Banhado transects (T2 and T3) are clearly lower than those from the Carandazal soils (T1), changing from 0.0 to 0.2 dS m^{-1} in the former and from 0.1 to 1.3 dS m^{-1} in the latter, with the exception of one surface sample (A2) at T3, from the bottom of the lake (P4), which has an atypical value of 51.0 dS m^{-1}. Vertically, EC_s tends to be greater in the deeper horizons of each profile (Bnc1, Bnc2, Bw4) of T1 and T3, but in a clearer way in the former transect. No evident pattern of lateral variation is observed along the three transects.

The Cation Exchange Capacity (CEC) is highly variable, and no apparent pattern of vertical and lateral distribution is noticed in the transects. The values change from 9.8 to 252.1 $mmol_c\ kg^{-1}$ in the Carandazal transect (T1), 7.1 to 74.8 $mmol_c\ kg^{-1}$ in the Cerca transect (T2) and 2.6 to 178.4 $mmol_c\ kg^{-1}$ in the Banhado transect (T3), but most of the samples at T1 and T2/T3 are, respectively, higher and lower than 60 $mmol_c\ kg^{-1}$ (Table 1). Along T1, the most abundant exchangeable cations are Ca^{2+} and Na^+, the latter being predominant only in Bnc1 and Bnc2 of higher positions. At T2 and T3, H^+ dominates near the surface, generally in the horizons A1, A2 and AB, whereas Ca^{2+} is the most abundant cation in all the other horizons (Table 1).

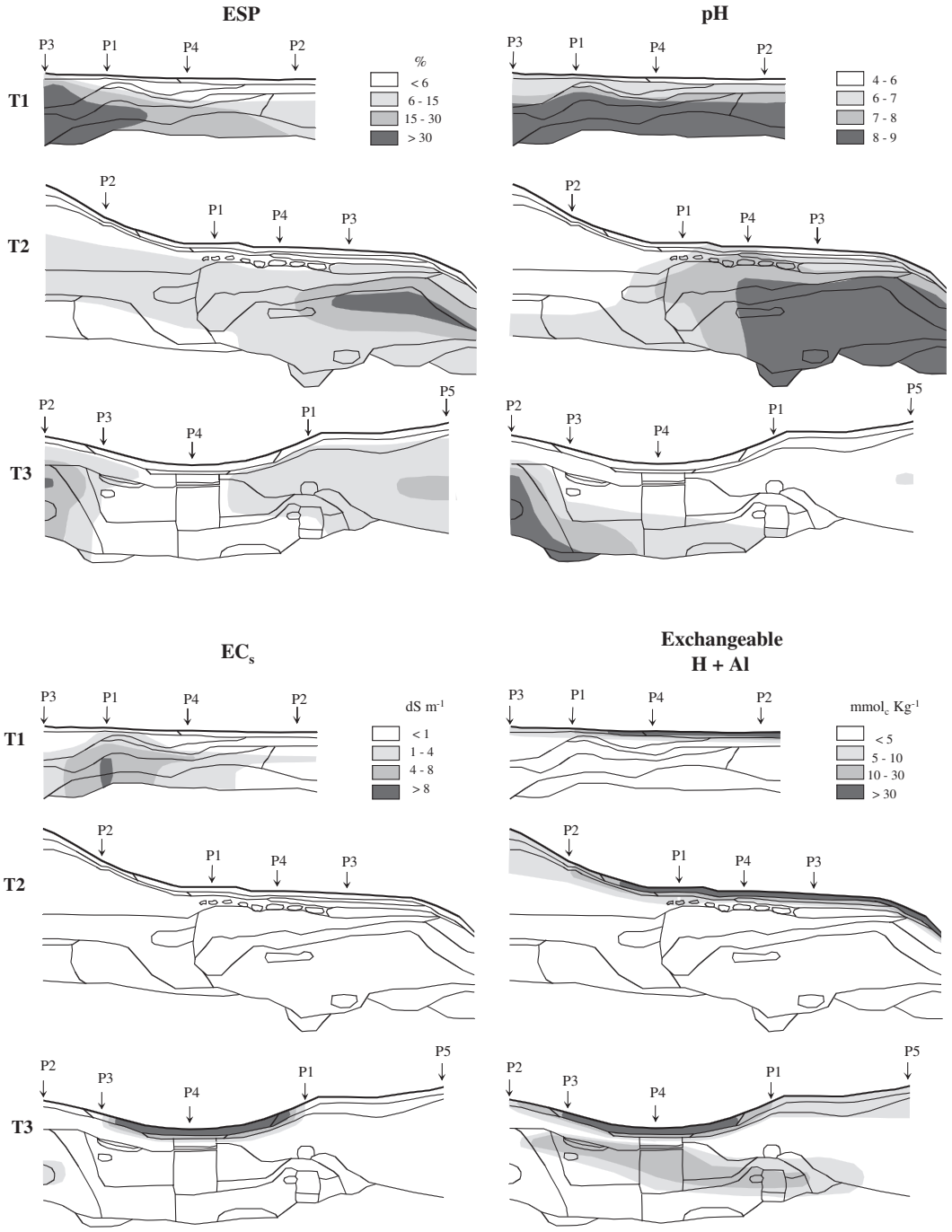

Fig. 4. Variation of Exchangeable Sodium Percentage (ESP), pH-H_2O, Electrical Conductivity in the saturated paste (Ecs) and Exchangeable H + Al along Transect 1 (T1 – Carandazal lake), Transect 2 (T2 – Cerca lake) and Transect 3 (T3 – Banhado lake). The black lines within the transects represent horizons boundaries.

Al^{3+} saturation is clearly lower in the Carandazal transect (T1), varying between 0.0 and 0.4% at T1, with most of the values equal to 0.0. The values change from 0.0% to 39.2% in the Cerca (T2) and from 0.0 to 19.0% in the Banhado transect (T3), but percentages higher than 5% are more common in the latter (Table 1). The majority of values of H + Al are between 0.0 and 55.0 $mmol_c\ kg^{-1}$ in the three transects, with the exception of only one higher number (93.6 $mmol_c\ kg^{-1}$) registered at T3 (A2, P4) (Table 1, Fig. 4). Both Al^{3+} saturation and H + Al tend to decrease downward in the profiles, being higher in the A1, A2, AB and Bw1 horizons. Laterally, the pattern of distribution of Al^{3+} saturation and H + Al is not well defined in the transects, although higher values of H + Al always occur near or at the center of the lake.

The base saturation changes from 57.0 to 100.0% at T1, 27.3 to 100.0% at T2 and 43.3 to 100.0% at T3 (Table 1). Unlike Al^{3+} saturation and H + Al, the base saturation clearly increases toward deeper horizons, with the smallest percentages at A1, A2, AB, Bw1. Lateral patterns are not evident, but the sandy zones of T2 (P2) and T3 (P5) have consistently lower percentages than other zones of the transects. The most abundant exchangeable base is Ca^{2+}, with Na^+ or K^+ being dominant only in some horizons (Table 1).

Although Na^+ is not the predominant base, the exchangeable sodium percentage (ESP) reaches 15% or more in horizons of all transects, but these high values are relatively more frequent at T1 (Table 1, Fig. 4). Considering each profile, ESP tend to be higher in deeper

Table 2
Chemical parameters measured from the saturated paste extract in selected samples.

Horizons	pH_s	EC_s dS m^{-1}	Ca^{2+} $mmol_c$ L^{-1}	Mg^{2+}	Na^{+}	SAR
Transect 1 – T1 (Carandazal lake)						
Pedon 3 (P3)						
A1	9.00	0.48	1.42	0.07	0.05	0.06
AB	6.86	0.08	0.20	0.00	0.07	0.21
Bnc2	8.89	1.84	0.40	0.29	9.37	15.91
Bnc1	8.60	2.00	0.74	0.64	19.63	23.60
Pedon 1 (P1)						
A1	7.85	0.62	2.49	1.00	0.41	0.31
Bw1	7.36	2.10	0.30	0.00	0.14	0.35
Bnc2	8.43	5.00	2.54	0.29	33.97	28.56
Bnc1	8.30	8.30	0.22	0.12	56.04	135.17
Bnc2	8.46	8.40	1.73	0.29	43.81	43.65
Pedon 4 (P4)						
A2	6.79	0.00	1.57	0.83	0.17	0.15
AB	7.65	0.19	0.40	0.00	0.15	0.33
Bw1	7.19	0.35	0.85	0.38	0.62	0.79
Bnc2	8.85	4.20	0.50	0.16	28.20	49.38
Bnc1	8.62	1.99	0.55	0.65	87.38	113.01
Bnc2	7.82	1.44	0.65	0.25	10.24	15.22
Pedon 2 (P2)						
A2	7.42	0.91	1.67	1.34	0.02	0.02
Bw1	7.89	0.33	0.85	0.28	0.32	0.42
Bw3	8.21	1.07	0.68	0.46	7.87	10.42
Bnc2	7.77	0.48	0.13	0.00	4.52	17.77
Transect 2 – T2 (Cerca lake)						
Pedon 2 (P2)						
A1	6.66	0.13	0.10	0.12	0.09	0.28
C1	5.38	0.05	0.05	0.14	0.08	0.28
C2	6.42	0.09	0.06	0.14	0.22	0.70
Bg1	5.12	0.09	0.20	0.06	0.18	0.51
Pedon 1 (P1)						
A2	6.73	0.05	0.60	0.06	0.17	0.30
Bnc1	6.12	0.02	0.34	0.13	1.38	2.86
Bnc2	6.72	0.14	0.25	0.11	0.87	2.07
Bnc1	6.36	0.03	0.34	0.12	1.11	2.30
Bnc2	6.32	0.03	0.32	0.20	0.07	0.13
Pedon 4 (P4)						
A2	7.24	0.05	0.49	0.09	0.15	0.28
Bw1	6.70	0.03	0.23	0.12	0.12	0.29
Bw2	7.62	0.03	0.33	0.10	0.26	0.55
Bnc1	8.26	0.04	0.25	0.12	0.56	1.31
Bnc2	8.19	0.06	0.22	0.24	2.38	4.94
Bnc1	8.04	0.05	0.14	0.18	2.30	5.68
Bnc2	7.88	0.07	0.23	0.31	3.23	6.23
Pedon 3 (P3)						
A2	7.27	0.08	0.53	0.03	0.15	0.28
Bw1	5.68	0.18	0.06	0.13	0.12	0.39
Bw2	6.19	0.12	0.05	0.14	0.12	0.38
Bnc1	5.38	0.03	0.03	0.05	0.70	3.51
Bnc2	7.90	0.04	0.17	0.11	0.87	2.33
Bnc1	8.13	0.11	0.67	0.60	4.53	5.69
Bnc2	8.73	0.10	0.44	0.51	5.65	8.21
Transect 3 – T3 (Banhado lake)						
Pedon 2 (P2)						
A1	6.74	0.19	0.14	0.23	0.07	0.16
AB	7.00	0.05	0.04	0.03	0.06	0.30
Bnc1	8.48	0.70	0.13	0.10	3.03	9.06
Bnc2	8.84	1.30	0.05	0.11	10.66	38.08
Bnc1	8.80	0.80	0.12	0.13	6.22	17.67
Pedon 3 (P3)						
A2	6.77	0.35	0.32	0.79	0.05	0.07
AB	6.33	0.08	0.11	0.03	0.13	0.51
Bc	5.86	0.38	0.10	0.13	3.04	8.95
Bw1	5.86	0.18	0.05	0.12	1.35	4.58
Bc	5.58	0.48	0.15	0.26	2.91	6.39
Bnc2	7.73	0.87	0.54	0.94	4.60	5.35
Pedon 4 (P4)						
A2	6.04	51.00	1.13	1.05	0.23	0.22
Bw1	5.35	0.31	0.44	0.60	0.35	0.48
Bc	5.65	0.34	0.45	0.60	0.80	1.11
Bw4	5.13	0.48	0.23	0.61	1.73	2.66
Bnc1	6.85	0.73	0.69	0.90	1.74	1.95

(continued on next page)

Table 2 (*continued*)

Horizons	pH_s	EC_s dS m^{-1}	Ca^{2+} $mmol_c$ L^{-1}	Mg^{2+}	Na^{+}	SAR
Pedon 1 (P1)						
A1	5.14	0.57	0.24	0.78	0.10	0.14
C1	6.74	0.12	0.05	0.01	0.23	1.31
Bw1	5.66	0.15	0.08	0.05	0.99	3.77
Bnc2	5.55	0.20	0.05	0.05	1.35	5.96
Bw5	5.76	0.22	0.03	0.01	1.13	8.04
Bg1	7.26	0.26	0.09	0.06	0.65	2.39
Pedon 5 (P5)						
A1	5.64	0.27	0.39	0.78	0.06	0.08
C1	6.93	0.11	0.02	0.06	0.27	1.30
C1	6.80	0.05	0.01	0.05	0.03	0.20

horizons, especially in Bnc1 and Bnc2. Laterally, toward the lake, the percentages tend to decrease at T1/T3 (P2 to P4) and increase at T2. The sodium adsorption ratio (SAR) is clearly larger at T1 compared to the T2 and T3 transects, with many more values higher than 13 in the former (Table 2). A clear difference between shallow (A1, A2, AB) and deep horizons (Bnc1, Bnc2, Bg1, Bw5) can be noted in the three transects, the deep having higher values. Laterally, SAR tends to increase toward the center of the depression at T2, but this pattern is not evident in the other transects. However, P2 of T3, located near the sand hill, has a much higher SAR than the other pedons of this transect.

4. Discussion

4.1. Degrees of transformation of the B horizons

Horizons Bnc1, Bnc2 and Bc of the three transects present morphological similarities to the olive and extremely hard Bnx of the saline lakes (Furquim, 2007; Furquim et al., 2008), such as a subsurface position, a greenish matrix (Bnc1 and Bnc2), a higher clay content than upper horizons and distinguished hardness. The laboratorial results of these B horizons also reveal the closest characteristics to the Saline-Sodic soils, inasmuch as they generally present the highest values of pH, EC_s, base saturation and ESP and the lowest values of Al^{3+} saturation and exchangeable H + Al. Commonly, these horizons have pH values that are classified as alkaline or strongly alkaline and ESP > 15%, which are typical attributes of salt-affected soils. These properties suggest that Bnc1, Bnc2 and Bc are genetically related to the soils originally formed around the saline lakes and represent transformations due to the geochemical changes of the lakes caused by the entrance of freshwater.

Additionally, the morphological and chemical differences between these B horizons insinuate different stages of transformation from the Bnx. The respective dominance of the hue 5Y, 2.5Y and 10YR in the matrix of Bnc1, Bnc2 and Bc, the higher variability of color and texture of the Bnc2 (four subhorizons) and Bc (two subhorizons) and the lower hardness of the Bc indicate that Bnc1 experienced the least and Bc experienced the most dramatic transformations. The analytical data partially corroborate this hypothesis because horizons Bnc1 and Bnc2 are not significantly different from each other, but both have properties that are more related to the salt-affected soils than the Bc, such as a higher pH and ESP and lower exchangeable Al^{3+} and H + Al.

Generic characteristics of the transects also indicate different degrees of transformation between them. In the Carandazal (T1), where the lake water is closer to the saline lakes (higher pH and EC), the soil distribution seems less complex, as in the Saline-Sodic soils, with Bnc1 and Bnc2 occurring in a vertical and lateral continuity. In the Cerca (T2), where the lake water has intermediate geochemistry characteristics (pH and EC), Bnc1 and Bnc2 tend to be vertically discontinuous, suggesting that the latter has replaced the former. Finally, the Banhado (T3), where the lake water is similar to the freshwater lakes (lower pH and EC), is the only transect to have the Bc, with Bnc1, Bnc2 and Bc appearing in lateral and vertical discontinuity. Moreover, the soils show a decrease in pH and an increase in Al^{3+} saturation from T1 to T2 and, then, to T3 and clearly higher values of EC_s, ESP and SAR at T1, indicating a higher chemical resemblance of this transect with the saline lake soils.

4.2. General processes and classification of the salt-affected soils

Salt-affected soils have been traditionally classified according to their values of electrical conductivity in the saturated paste (EC_s), exchangeable sodium percentage (ESP) and pH. Saline soils (Solonchak) are usually characterized by $EC_s \geq 4$ dS m^{-1} at 25 °C, ESP < 15% and a pH generally lower than 8.5, whereas Sodic soils (Solonetz) have $EC_s <$ 4 dS m^{-1}, ESP ≥ 15% and a pH ordinarily higher than 8.5. Saline-Sodic soils are intermediate, presenting $EC_s \geq 4$ dS m^{-1} and ESP ≥ 15%, as in the Saline and Sodic soils, respectively (USSL Staff, 1954; Sparks, 2003).

As previously described (item 2.1), the Saline-Sodic soils typically formed around the saline lakes contain $EC_s > 10$ dS m^{-1}, ESP > 30%, pH commonly higher than 10 and lack of exchangeable Al^{3+} and H + Al in the whole profile, indicating the action of salinization and solonization processes, the latter playing a more relevant role. All the soils studied in the present work have smaller EC_s, ESP and pH values and higher Al^{3+} saturation and exchangeable H + Al than the Saline-Sodic soils. In addition, they are chemically less homogeneous, inasmuch as many parameters show important vertical variation in the profiles. In the Carandazal transect (T1), Bnc1 and Bnc2 have ESP > 15%, pH close to or higher than 8.5 and Ca^{2+} or Na^{+} as the dominant exchangeable cations. In contrast, near-surface horizons, such as A1, A2, AB and Bw1, present lower ESP and pH, with higher values of H + Al and a prevalence of exchangeable Ca^{2+}. Along the Cerca (T2) and Banhado (T3) transects, only the deeper horizons of P3 and P2, respectively, have ESP > 15 combined with pH values near or higher than 8.5, with Ca^{2+} or K^{+} as the main exchangeable cations. Neither the surface nor subsurface horizons of the other profiles, with a few exceptions, have the chemical criteria of Saline (Solonchak), Sodic (Solonetz) or Saline-Sodic soils.

These chemical attributes indicate that the action of salinization and solonization in the Saline-Sodic soils has been replaced by the solodization process in the studied areas, with leaching of exchangeable bases, including Na^{+}, their replacement by Al^{3+} and H^{+} and a consequent decrease in pH. It occurs first in the near-surface horizons, but tends to extend to higher depths in many pedons, especially of transects T2 and T3. This is expected for solodization, which tends to initiate in the upper profile, mainly in the A/B boundary, reaching the whole profile in the final stages (USSL Staff, 1954; Schaetzl and Anderson, 2005). Thus, the Saline-Sodic soils of the saline lakes are apparently transforming into Solonetz and/or degraded Solonetz (Solodized Solonetz and/or Solods) in and around the brackish lakes.

In chemical terms, the differences considered in the literature between Solonetz, Solodized Solonetz and Solods reflect the increase of leaching, with a gradual decrease of ESP, SAR and pH from the former

to the latter. Commonly, B horizons of Solonetz and Solodized Solonetz have, respectively, ESP > 15% and >10%, SAR > 13 and <13, pH > 8 and from 6 to 8.5. Compared to the B horizons, near-surface horizons may have higher, equal, or lower values of these parameters in the Solonetz, but generally present lower values in the Solodized Solonetz. Finally, Solods are characterized by ESP < 10% and SAR < 13, but the pH is highly variable, being usually acid to neutral in the upper horizons and neutral to alkaline in the B (Whittig, 1959; Hallsworth and Waring, 1964; Cairns and van Schaik, 1968; Sandoval and Reichman, 1971; Parakshin, 1984; Heck and Mermut, 1992; Mahjoory, 1979; Qadir et al., 2000; Zaidel'man et al., 2010). According to these characteristics, three pedons of T1 (P3, P1, P4) and one pedon of T3 (P2) are classified as Solonetz; one pedon of T1 (P2), two pedons of T2 (P4, P3) and one of T3 (P5) may be considered Solodized Solonetz; and two pedons of T2 (P2, P1) and three of T3 (P3, P4, P1) would be Solods.

In terms of Soil Taxonomy (Soil Survey Staff, 2014), all the studied soils are classified as Entisols, being Typic Udorthents (T1, P3; T3, P2) or Typic Quartzipsamments (T2-P2; T3-P5) at the higher positions and Aquic Udorthents at the lower positions of the transects (T1-P1, P4, P2; T2-P1, P4, P3; T3-P3, P4, P1). This classification does not reflect the salt-affected conditions and the processes of genesis of the studied soils. Thus, in accordance with other recent studies (Qadir et al., 2000; Zaidel'man et al., 2010; Miller and Brierley, 2011; Lyubimova et al., 2014), the terms Solonetz, Solodized-Solonetz and Solods were adopted to designate the studied soils, showing direct correspondence with the pedogenetic mechanisms identified in the area.

The classification of the studied soils as Solonetzes, Solodized Solonetzes and Solods corroborates the progressively higher degrees of transformation of the three transects in relation to the Saline-Sodic soils, as noted before (item 4.1). Leaching increases from T1 to T2 and, finally, to T3, the former having the highest number of Solonetzes and the latter having the highest number of Solod profiles. This trend shows that solodization is incipient in the Carandazal soils and is gradually in a more advanced stage in the Cerca and Banhado transects. Because it is in consonance with the decrease of water pH and EC_s from Carandazal (near to saline lakes) to Cerca and, then, to Banhado (near to freshwater lakes), the process has been likely caused by an atypical input of freshwater into these lakes, which used to have saline waters.

4.3. Relationship between solodization and the fluvial dynamics in the Nhecolândia

In the study area, soil leaching occurs due to the advancement of intermittent watercourses into the sand hills, ultimately creating new intermittent freshwater channels. Preserved saline lakes are fully surrounded by forested savanna (Almeida et al., 2003) and isolated within the sand hills, whereas the borders of the brackish lakes are partially deforested and somehow connected to the intermittent watercourses. This can be visualized in Fig. 1b, which shows: i) an elongated and narrow channel starting at the Carandazal lake and almost linked to the nearest intermittent watercourse; ii) extensive clearings and many irregular connections with large zones subjected to floods around the Cerca lake; and iii) a long, narrow and better developed channel, totally united to the intermittent watercourse, crossing the Banhado lake.

The aerial view demonstrates that the floor of Carandazal and Banhado lakes are located in the thalweg of the incipient channels, where freshwater flows more frequently, providing greater potential for leaching (Fig. 1b). A downslope decrease in pH and/or ESP along T1 and T3 and the development of more degraded soils at the center of lake (Solodized Solonetz at T1 and Solod at T3) are evidence of higher leaching in the lowest areas. Parakshin (1984), Anderson (2010), Zaidel'man et al. (2010) and Miller and Brierley (2011) also reported degraded Sodic soils (Solodized Solonetz and/or Solods) in lower positions of the landscape, but the mechanisms triggering solodization in these studies are generally related to intermittent waterlogging, a deep water table and downward solution percolation.

Although the Cerca lake is not inserted in a defined and elongated channel, the important connections with large flooding zones have likely allowed for high amount of seasonal freshwater input, which dilutes the soil solutions and promotes overall leaching, leading to the transformation of Saline-Sodic into degraded Sodic soils. This non-linear water entrance, however, seems to prevent higher rates of leaching in the lowest zones of the transect, which is demonstrated by an increase of pH and ESP toward the bottom of the depression and the presence of less degraded soils (Solodized Solonetz) in the lowest areas, in comparison to the soils occurring upslope (Solods). Because of the presence of the near-impervious Bnc and Bc horizons, a lateral subsurface flow of water and soluble salts is expected over these horizons, triggering seasonal water stagnation and ion accumulation in the lower zones. Then, leaching is improved upslope, especially in the upper horizons, creating Solods, whereas accumulation of ions occurs downslope, with the genesis of Solodized Solonetz in lower positions. Miller and Pawluk (1994) and Miller and Brierley (2011) also observed more Na-enriched soils (Solodized Solonetz or Solonetz) in the depressed areas of the landscape, mainly due to lateral flow of bases and waterlogging as a result of poorly permeable horizons and/or a shallow water table.

Typical alluvial fan processes control the drainage development and water dynamics in the low Nhecolândia. Alluvial fans, such as the Taquari megafan, are primarily built by the formation and abandonment of depositional lobes (Assine, 2003; Assine and Silva, 2009), which are defined as elongated patterns originated by active deposition of sediments by a drainage network (Zani et al., 2009). These drainage systems are mainly comprised of distributary channels, which have an opposite behavior from the common tributary channels, inasmuch as they flow away from a larger river (Assine, 2003; Schumm, 1977). The current depositional lobe of the Taquari River is located in the central and distal zone of the megafan, outside the Nhecolândia, where only abandoned lobes are present (Assine et al., 2005; Zani et al., 2006).

Erosional processes commonly operate in inactive lobes, impressing degradational features over previous aggradational landforms (Zani et al., 2009). In the low Nhecolândia, intermittent watercourses are recognized as current tributary channels that overprint, by erosional processes, the typical distributary paleochannels of the abandoned lobes (Assine, 2003). Then, periodic flooding in the intermittent watercourses has likely amplified and ultimately formed new channels, such as those involving Carandazal and Banhado lakes, provoking partial or full erosion of local sand hills. Fernandes (2007) also observed embayed and non-linear forms in the borders of sand hills caused by erosion of intermittent watercourses, coupled with erosional features formed by runoff immediately around saline lakes, after intense precipitation. These processes are likely responsible for the irregular connections between the Cerca lake and the nearest intermittent watercourses. Thus, linear or non-linear erosion of the sand hills are responsible for the connection of the saline lake to the seasonal freshwater inundation and, consequently, its transformation into brackish lakes.

The precise beginning of this transformation is still unknown. Based on sediment thermoluminescence and ^{14}C dating mainly from the Taquari megafan, Assine (2003) suggests that the Pantanal wetland, as currently known, developed in the Pleistocene/Holocene transition, when the climate became more humid. According to this author, the rise in precipitation rates raised the water table in the early Holocene, creating lakes in ancient deflation depressions, previously formed due to the prevalence of a dry climate during the Late Pleistocene. The higher water availability would also enable the connection between many of these lakes and the formation of intermittent watercourses, whereas other lakes would remain isolated in the low Nhecolândia, becoming progressively saline. Whitney et al. (2011), through fossil pollen and diatom data from lake sediments in the northern Pantanal, show a marked drier climate during the late Pleistocene (45,000 to 19,500 years BP) and a clear increase in the precipitation rates in the Pleistocene/Holocene transition (~12,200 years BP), corroborating the assumptions of Assine (2003).

During the Holocene, however, the Pantanal wetland passed through a moderate drought period that lasted, according to Whitney et al. (2011), from 10,000 to 3000 years BP and, according to McGlue et al. (2012), from 5300 to 2600 years BP. The former study, based on sediment radiocarbon dating of shallow lakes in the central-northern Pantanal, also concluded that this period confined the Paraguay River to its channel and, only approximately 2600 years BP, a regular flood regime and strong inundation pulse begin to occur in the wetland. Additionally, in Bonito County, near the Nhecolândia but outside the Pantanal, recurrent dry events were registered in speleothems dating from 3800 to 2600 years BP, with an increase in rainfall starting after this period (Bertaux et al., 2002). Although complete agreement is not achieved in the literature, it seems that in the last 2500–3000 years the Pantanal has experienced a clear increase in moisture levels.

This higher water availability during the Late Holocene has likely provoked the transformation of saline into brackish lakes, with important expansion of the intermittent watercourses and erosion of the sand hills. Therefore, the fluvial erosive dynamics in the Nhecolândia in the last 2500–3000 years are apparently the main explanation for the degradation of the Saline-Sodic soils, promoting the replacement of solonization by solodization in and around the brackish lakes. Consequently, Saline-Sodic soils are transformed mainly into Solonetz in and around more mineralized lakes (Carandazal) and into Solodized Solonetz or Solods in and around less mineralized lakes (Cerca and Banhado).

4.4. Local processes in the studied soils

Because salt-affected soils tend to occur in near-flat or depressed areas, the stagnation of water during at least part of the year tends to trigger hydromorphic processes, which assume a complementary role in their genesis (Miller and Brierley, 2011). Horizons Bg1, Bg2, BA and Bw4 have been affected by redox conditions, which is evidenced by typical gley colors and deep positions in the profiles, where water stagnation is longer, or location in the lowest zone of the lake depression, where water reaches shallow horizons during the wet season (Vepraskas, 1996; Vepraskas, 2001; van Breemen and Buurman, 2003).

The deep horizons Bg1 and Bg2 are apparently transforming from Bnc or Bc horizons because they are vertically or laterally contiguous and have similar clay-enriched textures. Additionally, nodules similar in color and consistency to the greenish and hard Bnc1 are commonly found in these horizons, suggesting a genetic relationship between them. Homogeneous change from grayish to light brownish colors coupled with an increase in chroma after drying was observed in all samples (not shown), which suggests that both horizon Bg1 and Bg2 have a reduced matrix with the occurrence of Fe^{2+} and its oxidation to Fe^{3+} when exposed to air. However, the dominance of coarser textures in most of the samples compared to the adjacent Bnc and Bc horizons also indicates a partially clay-depleted matrix (Vepraskas, 1996; Vepraskas, 2001).

The fine clay fraction of the B horizons around the saline lakes is mainly composed of neoformed Fe-rich micas (ferric illite and glauconite types). Fe^{3+} and Al^{3+}- Fe^{3+} are the main cations in the octahedral sheet of glauconites and ferric illites, respectively (Furquim et al., 2010b). Mineralogical analyses in progress (not shown) revealed that similar ferruginous micas are present in the Bnc and Bc horizons of the studied area. Reduction of Fe^{3+} to Fe^{2+} within the Fe-micas, triggered by microbial respiration, is likely responsible for their dissolution and the consequent diffusion of Fe^{2+} through the matrix, providing a generalized gray color in horizons Bg1 and Bg2 (Vepraskas, 2001). Experiments have shown that illite dissolution by iron bioreduction depends on Fe^{3+} contents within the structure, being efficient only if the phases are highly ferruginous (Vodyanitskii, 2007), such as the micas formed around the saline lakes. This is, thus, an important mechanism of destruction of the Bnc and Bc horizons in the studied lakes. Ultimately, this mechanism may be responsible for the transformation of these horizons into the sandy C horizons, which are similar to the sandy and unconsolidated material that has filled the sedimentary basin during the Cenozoic (Del'Arco et al., 1982; Godoi Filho, 1986). Evidence of this transformation may be found in Transect 2 (T2), where a discontinuous Bcn1 is intermingled with the C1 near the surface (P1 to P3) and a remnant Bnc1 is adjacent to both a Bg1 and a large and isolated volume of C2 in deep positions of the profiles (P2 and surroundings).

The redoximorphic features found in horizons BA and Bw4, both located in the bottom of the lake, are mostly red or orange concentrations of Fe oxides or hydroxides (Vepraskas, 1996; Vepraskas, 2001; Schaetzl and Anderson, 2005), with circular or linear shapes and in general related to root channels. These features, which are rarely to abundantly distributed in the matrix, confirm seasonal fluctuations of the water table in these shallower horizons (van Breemen and Buurman, 2003). A laboratory experiment performed by Vepraskas and Bouma (1976) over 150 days attested to the formation of iron mottles in cores under a saturated regime and with low redox potentials for a longer time.

The genesis of horizons BA and Bw4, accompanied by horizon Bw3, seem to also be related to the sedimentation dynamics of the lakes. They have a more clayey texture than the contiguous upslope horizons (AB for BA, Bnc1 for Bw3 and Bnc1, Bnc2 and Bc for Bw4). Additionally, horizons Bw3 and Bw4 present the same volumes found in the Bnc and Bc horizons, such as the black nodules and greenish (5Y and 2.5Y) masses. Thus, horizons BA, Bw3 and Bw4 are likely derived from previous AB, Bnc and Bc horizons and have been transformed as a consequence of colloid deposition from the low energy pond that seasonally accumulates in the most depressed zones. The marked decrease in value and chroma of horizon Bw3 if compared to their upslope neighbors suggests that not only clay minerals but also organic matter have been aggregated into the matrix.

5. Conclusions

Degraded Sodic soils associated with ephemeral brackish lakes in the low Nhecolândia occur in a sequence of evolution that is strictly related to the water geochemistry. Solonetzes are prevalent in and around the Carandazal lake, which has the closest pH and EC to the saline lakes; Solods are more common in and around the Banhado lake, which has the closest pH and EC to the freshwater lakes; and both Solodized Solonetz and Solods are equally distributed in and around the Cerca lake, which has intermediate water characteristics. This consistent relationship is associated with atypical freshwater input within the sand hills, leading to the transformation of the saline lakes into brackish lakes. In the Carandazal and Banhado lakebeds and their surroundings, the freshwater entrance clearly occurs through the formation of new intermittent watercourses, a feature that is easily perceived via aerial photography.

The transformation of soils associated with saline lake degradation occurs mainly through intense leaching, first in the near-surface horizons (Solonetz, Solodized Solonetz) and later in the whole profile (Solods), which is characteristic of the solodization process. It occurs to higher degrees along the thalweg of the intermittent watercourse in the Carandazal and Banhado lakes and in the higher areas of the transect associated with the Cerca lake. To our knowledge, the connection between the evolution of salt-affected soils and current fluvial dynamics has not been broached in the international literature. Then, the recent genesis of intermittent watercourses can be considered a new mechanism of genesis of Sodic (Solonetz) and degraded Sodic soils (Solodized Solonetz and Solods), especially in alluvial fan environments.

The results of this research suggest that the saline lakes, which only occur in the low Nhecolândia subregion, have been destroyed and ultimately replaced by freshwater lakes. This implies that the region has passed through a general desalinization, which probably occurred in the last 3000 years, when the climate apparently became more humid in the wetland. Previous research (Barbiéro et al., 2002; Furquim et al., 2010a) has proven that the evaporative concentration of waters is

currently occurring in the preserved saline lakes, maintaining their water characteristics. However, once the isolation of the saline lake is interrupted, with recurrent freshwater input, this equilibrium is likely disrupted and the degradation process is apparently irreversible.

Acknowledgments

The authors wish to thank FAPESP for the financial support to the research (Project 2011/22491-0) and for the fellowship to T.T.V.N., CAPES for the fellowship to M.A.B., CNPq for the fellowship to M.A.S., technicians of UNIFESP, campus Diadema, for help with the laboratory work and employees of the Nhumirim Farm (EMBRAPA) for their assistance in the field.

References

Adámoli, J., 1986. A dinâmica das inundações no Pantanal. Anais do 1° Simpósio sobre Recursos Naturais e Sócio-Econômicos do Pantanal, 27/11 a 04/12/1984, Corumbá (MS), pp. 51–61.

Alfonsi, R.R., Camargo, M.B.P., 1986. Condições climáticas para a região do Pantanal Matogrossense. Anais do 1o Simpósio sobre Recursos Naturais e Sócio-Econômicos do Pantanal, 27/11 a 04/12/1984, Corumbá (MS), pp. 29–42.

Almeida, T.I.R., Sígolo, J.B., Fernandes, E., Queiroz Neto, J.P., Barbiero, L., Sakamoto, A.Y., 2003. Proposta de Classificação e Gênese das Lagoas da Baixa Nhecolândia-MS com Base em Sensoriamento Remoto e dados de campo. Revista Brasileira de Geociências 33, 88–90.

Almeida, T.I.R., Karmann, I., Paranhos Filho, A.C., Sígolo, J.B., Bertolo, R.A., 2010. Os diferentes graus de isolamento da água subterrânea como origem de sua variabilidade: evidências isotópicas, hidroquímicas e da variação sazonal do nível da água no Pantanal da Nhecolândia. Revista Brasileira de Geologia 10, 37–47.

Alvarenga, S., Brasil, A., Pinheiro, R., Kux, H., 1984. Estudo Geomorfológico Aplicado à Bacia do Alto Rio Paraguai e Pantanais Matogrossenses. Boletim Técnico Projeto Radambrasil- Série Geomorfologia. 1 (187 p.).

Anderson, D., 2010. Solonetzic soils of the Prairie region. PS&C Prairie Soils & Crops Journal 3, 65–72.

Assine, M.L., 2003. Sedimentação na Bacia do Pantanal Mato-Grossense, Centro-Oeste do Brasil. UNESP, Instituto de Geociências e Ciências Exatas, Rio Claro (Tese de Livre-Docência, 106 p.).

Assine, M.L., 2015. Brazilian Pantanal: a large pristine tropical wetland. In: Vieira, B.C., Salgado, A.A.R., Santos, L.J.C. (Eds.), Landscapes and landforms of Brazil. Springer, pp. 135–146.

Assine, M.L., Silva, A., 2009. Contrasting fluvial styles of the Paraguay River in the northwestern border of the Pantanal wetland, Brazil. Geomorphology 113, 189–199.

Assine, M.L., Padovani, C.R., Zacharias, A.A., Ângulo, R.J., Souza, M.C., 2005. Compartimentação geomorfológica, processos de avulsão fluvial e mudanças de curso do Rio Taquari, Pantanal Mato-Grossense. Revista Brasileira de Geomorfologia 6, 97–108.

Assine, M.L., Merino, E.R., Pupim, F.P., Macedo, H.A., Santos, M.G.M., 2015. The Quaternary alluvial systems tract of the Pantanal Basin, Brazil. Brazilian Journal of Geology 45 (3), 475–489.

Bacani, V.M., Sakamoto, A.Y., Quénol, H., Vannier, C., Corgne, S., 2016. Markov chains–cellular automata modeling and multicriteria analysis of land cover change in the Lower Nhecolândia subregion of the Brazilian Pantanal wetland. J. Appl. Remote. Sens. 10 (1), 1–20.

Barbiéro, L., Queiroz Neto, J.P., Sakamoto, A.Y., 2000. Características Geoquímicas dos Solos Relacionadas à Organização Pedológica e à Circulação da Água (Fazenda Nhumirim: Embrapa CPAP, Nhecolândia, MS). Anais do 3o Simpósio sobre Recursos Naturais e Sócio-Econômicos do Pantanal, Corumbá (MS), pp. 90–100.

Barbiéro, L., Furian, S., Queiroz Neto, J.P., Ciornei, G., Sakamoto, A.Y., Capellari, B., Fernandes, E., Valles, V., 2002. Geochemistry of water and ground water in the Nhecolândia, Pantanal of Mato Grosso, Brazil: variability and associated processes. Wetlands 22, 528–540.

Barbiero, L., Rezende Filho, A., Furquim, S.A.C., Furian, S., Sakamoto, A., Valles, V., Graham, R., Fort, M., Dias Ferreira, R.P., Queiroz Neto, J.P., 2008. Soil morphological control on saline and freshwater lake hydrogeochemistry in the Pantanal of Nhecolândia, Brazil. Geoderma 148, 1–16.

Bertaux, J., Sondag, F., Santos, R., Soubiès, F., Causse, C., Plagnes, V., Le Cornec, F., Seidel, A., 2002. Paleoclimatic recordo f speleothems in a tropical region: study of laminated sequences from a Holocene stalagmite in Central-West Brazil. Quat. Int. 89, 3–16.

Bohn, H.L., McNeal, B.L., O'Connor, G.A., 2001. Soil Chemistry. 3rd edition. John Wiley and Sons, New York (322 p.).

Boulet, R., 1992. Uma Evolução Recente da Pedologia e suas Implicações no Conhecimento da Gênese do Relevo. Anais do III Congresso ABEQUA, pp. 43–51 Belo Horizonte.

Bui, E.N., Krogh, L., Lavado, R.S., Nachtergaele, F.O., Tóth, T., Fitzpatrick, R.W., 1998. Distribution of sodic soils: the world scene. In: Sumner, M.E., Naidu, R. (Eds.), Sodic Soils, Distribution, Properties, Management, and Environmental Consequences. Oxford University Press, pp. 3–17.

Cairns, R.R., van Schaik, J.C., 1968. Solonetzic soils and their physical properties as influenced by different cation. Can. J. Soil Sci. 48, 165–171.

Cantarella, H., van Raij, B., Coscione, A.R., Andrade, J.C., 2001. Determinação de Alumínio, Cálcio e Magnésio trocáveis em extrato de Cloreto de Potássio. In: Raij, B., Andrade, J.C., Cantarella, H., Quaggio, J.A. (Eds.), Análise Química para Avaliação da Fertilidade de Solos Tropicais. IAC, Campinas.

Carvalho, N., 1986. Hidrologia da Bacia do Alto Paraguai. Anais do 1o Simpósio sobre Recursos Naturais e Sócio-Econômicos do Pantanal, 27/11 a 04/12/1984, Corumbá (MS), pp. 43–49.

Costa, M., Telmer, K.H., Evans, T.L., Almeida, T.I.R., Diaku, M.T., 2015. The lakes of the Pantanal: inventory, distribution, geochemistry, and surrounding landscape. Wetl. Ecol. Manag. 23, 19–39.

Cunha, N.G., 1980. Considerações sobre os solos da sub-região da Nhecolândia, Pantanal Mato-Grossense. Circular Técnica Embrapa 1, 1–45.

Del'Arco, J.O., Silva, R.H., Tarapanoff, I., Freire, F.A., Pereira, L.G.M., Souza, S.L., Luz, D.S., Palmeira, R.C.B., Tassinari, C.C.G., 1982. Geologia da Folha SE.21 Corumbá e Parte da Folha SE.20. RADAMBRASIL-Levantamento dos Recursos Naturais. Rio de Janeiro, pp. 25–160.

EMBRAPA, Empresa Brasileira de Pesquisa Agropecuária, 1997. Manual de Métodos de Análise de Solo. 2ª edição. Centro Nacional de Pesquisa de Solos, Rio de Janeiro/RJ (Revisão atual. 212 p.).

Evans, T.L., Costa, M., 2013. Landcover classification of the lower Nhecolândia subregion of the Brazilian Pantanal wetland using ALOS/PALSAR, RADARSAT-2 and ENVISAT/ASAR imagery. Remote Sens. Environ. 128, 118–127.

Fanning, D.S., Fanning, M.C.B., 1989. Soil, Morphology, Genesis, and Classification. John Wiley & Sons, New York (395 p.).

Fernandes, E., 2000. Caracterização dos Elementos do Meio Físico e da Dinâmica da Nhecolândia (Pantanal Sulmatogrossense). Dissertação de Mestrado. Depto de Geografia, Faculdade de Filosofia, Letras e Ciências Humanas, Universidade de São Paulo (130 p.).

Fernandes, E., 2007. Organização espacial dos componentes da paisagem da Baixa Nhecolândia – Pantanal de Mato Grosso do Sul. Tese de Doutorado. Depto de Geografia, Faculdade de Filosofia, Letras e Ciências Humanas, Universidade de São Paulo (177 p.).

Furquim, S.A.C., 2007. Formação de Carbonatos e Argilominerais em Solos Sódicos no Pantanal Sul-Mato-Grossense. São Paulo/SP. Tese de Doutorado. 2007.

Furquim, S.A.C., Graham, R., Barbiéro, L., Queiroz Neto, J.P., Vallès, V., 2008. Mineralogy and genesis of smectites in an alkaline-saline environment of Pantanal wetland, Brazil. Clay Clay Miner. 56, 580–596.

Furquim, S.A.C., Graham, R.C., Barbiero, L., Queiroz Neto, J.P., Vidal-Torrado, P., 2010a. Soil mineral genesis and distribution in a saline lake landscape of the Pantanal Wetland, Brazil. Geoderma 518–528.

Furquim, S.A.C., Barbiéro, L., Graham, R.C., Queiroz Neto, J.P., Dias Ferreira, R.P., Furian, S., 2010b. Neoformation of micas in soils surrounding an alkaline-saline lake of Pantanal wetland, Brazil. Geoderma 158, 331–342.

Gedroiz, K.K., 1912. Colloidal chemistry as related to soil science. I. Colloidal substances in the soil solution. Formation of sodium carbonate in the soil. Alkali soil and saline soils. Zhurnal Opitnoii Agronomii 13, 363–420.

Gedroiz, K.K., 1917. Saline soils and their improvement. Zhurnal Opitnoii Agronomii. 18, 122–140.

Gedroiz, K.K., 1925. Soil absorbing complex and the absorbed soil cations as a basis of genetic soil classification. Nosovka Agricultural Experimental Station. 38 (Translation into English: S.A. Waksman).

Godoi Filho, J.D., 1986. Aspectos Geológicos do Pantanal Mato-Grossense e de sua Área de Influência. Anais do 1o Simpósio sobre Recursos Naturais e Sócio-Econômicos do Pantanal, 27 de novembro a 4 de dezembro de 1984, Corumbá (MS), pp. 63–76.

Góes, M.A.C., Luz, A.B., Possa, M.V., 2004. Amostragem. Comunicação Técnica CT2004-180-00. 19–51. Centro de Tecnologia Mineral (CETEM). Ministério da Ciência e Tecnologia, Rio de Janeiro.

Hallsworth, E.G., Waring, H.D., 1964. Studies in Pedogenesis in New South Wales. VIII. An alternative hypothesis for the formation of the solodized solonetz of the Pilliga disctrict. J. Soil Sci. 15, 158–177.

Hamilton, S.K., 1999. Potential effects of a major navigation project (Paraguay-Paraná Hidrovía) on inundation in the Pantanal floodplains. Regul. Rivers Res. Manag. 15, 289–299.

Hamilton, S.K., Sippel, S.J., Melack, J.M., 1996. Inundation patterns in the Pantanal wetland of South America determined from passive microwave remote sensing. Arch. Hydrobiol. 137 (1), 1–23.

Heck, R.J., Mermut, A.R., 1992. Genesis of Natriborolls (Solonetzic) in a close lake basin in Saskatchewan, Canada. Soil Sci. Soc. Am. J. 56, 842–848.

Janzen, W.K., Moss, H.C., 1956. Exchangeable cations in solodized solonetz and solonetz-like soils of Saskatchewan. J. Soil Sci. 7, 203–212.

Kellog, C.E., 1934. Morphology and genesis of the solonez soils of western South Dakota. Soil Sci. 38 (483-450).

Kisel, V.D., 1981. Origin of Ukrainian solonetzic soils. Soviet Sol Science 12, 16–22.

Lyubimova, I.N., Khan, V.V., Salpagarova, I.A., 2014. Diagnosis of solonetzic process in virgin and agrogenically transformed soils of different regions. Eurasian Soil Science 47, 863–872.

Mahjoory, R.A., 1979. The nature and genesis of some salt-affected soils in Iran. America Journal]–>Soil Sci. Soc. Am. J. 43, 1019–1024.

Martins, E.R.C., 2012. Tipologia de Lagoas Salinas no Pantanal da Nhecolândia (MS). Tese de Doutorado. USP/SP.

McBride, M.B., 1994. Environmental chemistry of soils. Cap.8, Salt-affected and Swelling Soils. Oxford University Press (18 p.).

McGlue, M.M., Silva, A., Zani, H., Corradini, F.A., Parolin, M., Abel, E.J., Cohen, A.C., Assine, M.L., Ellis, G.S., Trees, M.A., Kuerten, S., Gradella, F.S., Rasbold, G.G., 2012. Lacustrine records Holocene flood pulse dynamics in the Upper Paraguay River watershed (Pantanal wetlands, Brazil). Quat. Res. 78, 285–294.

Miller, J.J., Brierley, J.A., 2011. Solonetzic soils of Canada: genesis, distribution, and classification. Can. J. Soil Sci. 91, 889–902.

Miller, J.J., Pawluk, S., 1994. Genesis of solonetzic soils as a function of topography and seasonal dynamics. Can. J. Soil Sci. 74, 207–217.
Munn, L.C., Boehm, M.M., 1983. Soil genesis in a Natrargid-Haplargid complex in northern Montana. Soil Sci. Soc. Am. J. 47, 1186–1192.
Padovani, C.R., 2010. Dinâmica espaço-temporal das inundações no Pantanal. Escola Superior de Agricultura Luiz de Queiroz (Esalq), Universidade de São Paulo, Tese de Doutorado.
Parakshin, P.Y., 1984. Solonetzic soils of depressions of northern Kazakhstan. Soviet Soil Sci. 16, 9–16.
Parizotto, T.M., 2012. Estudo Morfológico e Hidroquímico de Pequenas Depressões na Nhecolândia, Pantanal, MS. Dissertação de Mestrado. Departamento de Geografia, Universidade de São Paulo.
Por, F.D., 1995. The Pantanal of Mato Grosso (Brazil) — World's Largest Wetlands. Klumer Ac. Publ. (122 p.).
Pott, A., Silva, J.S.V., 2016. Terrestrial and aquatic vegetation diversity of the Pantanal wetland. In: Bergier, I., Assine, M.L. (Eds.), Dynamics of the Pantanal Wetland in South America. Springer International Publishing, pp. 111–131.
Qadir, M., Ghafoor, A., Murtaza, G., 2000. Amelioration strategies for saline soils: a review. Land Degrad. Dev. 11, 501–521.
Quaggio, J.A., Raij, B., 2001. Determinação do pH em Cloreto de Cálcio e da Acidez Total. In: Raij, B., Andrade, J.C., Cantarella, H., Quaggio, J.A. (Eds.), Análise Química para Avaliação da Fertilidade de Solos Tropicais. IAC, Campinas.
Queiroz Neto, J.P., Sakamoto, A.Y., Lucati, H.M., Fernandes, E., Capellari, B., 1997. Solos de Cordilheiras, Baías e Lagoas salinas na Área do Leque (Pantanal da Nhecolândia, MS). Anais da VIII Semana de Estudos de Geografia do CEUL-UFMS, Três Lagoas (MS), pp. 16–20.
Rengasamy, P., Sumner, M.E., 1998. Processes involved in sodic behavior. In: Sumner, M.E., Naidu, R. (Eds.), Sodic Soils, Distribution, Properties, Management, and Environmental Consequences. Oxford University Press, pp. 35–50.
Rezende Filho, A.T., 2006. Estudo da Variabilidade e Espacialização das Unidade da Paisagem: Banhado (baía/vazante), Lagoa Salina e Lagoa Salitrada no Pantanal da Nhecolândia, MS. Dissertação de Mestrado. Universidade Federal de Mato Grosso do Sul, Campus Três Lagoas (109 p.).
Ruellan, A., Dosso, M., 1993. Regards sur le sol. Les Éditions Foucher. Universités Francophones, Paris.
Sakamoto, A.Y., 1997. Dinâmica hídrica em uma lagoa salina e seu entorno no Pantanal da Nhecolândia: contribuição ao estudo das relações entre o meio físico e a ocupação, Fazenda São Miguel Firme, MS. Tese de Doutorado. Departamento de Geografia da Faculdade de Filosofia, Letras e Ciências Humanas da Universidade de São Paulo (183 p.).
Sandoval, F.M., Reichman, G.A., 1971. Some properties of Solonetzic (Sodic) soils in western North Dakota. Can. J. Soil Sci. 51, 143–155.
Schaetzl, R.J., Anderson, S., 2005. Soils, Genesis and Geomorphology. Cambridge University Press, Cambridge (817 pp.).
Schoeneberger, P.J., Wysocki, D.A., Benham, E.C., Broderson, W.D., 2002. Field Book for Describing and Sampling Soils. Version 2.0. Natural Resources Conservation Service, National Soil Survey Center, Lincoln, NE.
Schumm, S.A., 1977. The Fluvial System. Wiley (338 p.).
Scott, D.A., 1991. Latin America and the Caribbean. In: Finlayson, C.M., Moser, M.E. (Eds.), Wetlands: A Global Perspective. Facts on File, New York, pp. 85–114.
Silva, T.C., 1986. Contribuição da Geomorfologia para o Conhecimento e Valorização do Pantanal. Anais do 1o Simpósio sobre Recursos Naturais e Sócio-Econômicos do Pantanal, 27 de novembro a 4 de dezembro de 1984, Corumbá (MS), pp. 77–90.
Silva, M.H., 2007. Subsídios para a compreensão dos processos pedogenéticos da lagoa Salitrada: Pantanal da Nhecolândia, MS. Dissertação de Mestrado. Universidade Federal do Mato Grosso do Sul (MS), Campus Aquidauana.
Silva, J.S.V., Abdon, M.M., 1998. Delimitação do Pantanal Brasileiro e suas Sub-regiões. Pesq. Agrop. Brasileira 33, 1703–1711.
Silva, M.H., Sakamoto, A., 2003. Perfis pedomorfológicos do Pantanal da Nhecolândia-MS: Um estudo comparativo. XII Encontro Sul-Matogrossense de Geografia, Três Lagoas, MS, pp. 544–552.
Silva, C.J., Wantzen, K.M., Nunes da Cunha, C., Machado, F.D.A., 2001. Biodiversity in the Pantanal Wetland, Brazil. In: Gopal, B., Junk, W.J., Davis, J.A. (Eds.), Biodiversity in Wetlands: Assessment, Function and Conservation 2. Backhuys Publishers, Leiden (pp. 187-21).
Silva, M.H., Sakamoto, Y.A., Barbiero, L., Queiroz Neto, J.P., Furian, S., 2004. Morfologia do solo de três topossequências na área da lagoa Salina do Meio, Fazenda Nhumirim, Pantanal da Nhecolândia, MS. IV Simpósio sobre Recursos Naturais e Sócio-Econômicos do Pantanal, Corumbá/MS, 23 a 26/11.
Silva, F.C., Abreu, M.F., Pérez, D.V., Eira, P.A., Abreu, C.A., van Raij, B., Gianello, C., Coelho, A.M., Quaggio, J.A., Tedesco, M.J., Silva, C.A., Cantarella, H., Barreto, W.O., 2009. Métodos de Análises químicas para fins de fertilidade do solo, Capítulo 1. In: Silva, F.C. (Ed.), Manual de Análises Químicas de Solos, Plantas e Fertilizantes, 2ª edição revista e ampliada, pp. 130–138.
Silva, J.S.V., Abdon, M.M., Silva, S.M.A., Moraes, J.A., 2011. Evolution of deforestation in the Brazilian Pantanal and surroundings in the timeframe 1976–2008. Geografia 36, 35–55.
Soil Survey Staff, 2014. Keys to Soil Taxonomy. 12th ed. USDA-Natural Resources Conservation Service, Washington, DC (362 p.).
Sparks, D.L., 2003. Environmental Soil Chemistry. 2nd edition. Academic Press, San Diego (352 p.).
Sumner, M.E., Rengasamy, P., Naidu, R., 1998. Sodic soils: a reappraisal. In: Sumner, M.E., Naidu, R. (Eds.), Sodic Soils, Distribution, Properties, Management, and Environmental Consequences. Oxford University Press, pp. 3–17.
Tarifa, J.R., 1986. O Sistema Climático do Pantanal: da compreensão do sistema à definição de prioridades de pesquisa climatológica. Anais do 1o Simpósio sobre Recursos Naturais e Sócio-Econômicos do Pantanal, 27 de novembro a 4 de dezembro de 1984, Corumbá (MS), pp. 9–27.
Torge, W., Muller, J., 2012. Geodesy. De Gruyter. 4th edition. (Berlin/Boston).
USDA, 2014. Soil Survey Field and Laboratory Methods Manual. United States Department of Agriculture Natural Resources, Conservation Services (NRCS) (Soil Survey Investigations Report No. 51, Version 2, 487 p.).
USSL Staff, 1954. Diagnosis and Improvement of Saline and Alkali Soils. 60. U. S. Department of Agriculture, United States Salinity Laboratory (USSL), Washington Handbook. (160 p.).
van Breemen, N., Buurman, P., 2003. Soil Formation. 2nd edition. Kluwer Academic Publ, New York.
Vepraskas, M.J., 1996. Redoximorphic features for identifying aquic conditions. Technical Bulletin 301. North Caroline Agricultural Research Service, Raleigh, NC (33 p.).
Vepraskas, M.J., 2001. Morphological features of seasonally reduced soils. In: Richardson, J.L., Vepraskas, M.J. (Eds.), Wetland Soils. Lewis Publishers, Boca Raton, pp. 163–182.
Vepraskas, M.J., Bouma, J., 1976. Model Experiments on mottle formation simulating field conditions. Geoderma 15, 217–230.
Vodyanitskii, Y.N., 2007. Reductive biogenic transformation of Fe (III)-containing phyllosilicates (review of publications). Eurasian Soil Science 40, 1355–1363.
Westin, F.C., 1953. Solonetz soils on eastern South Dakota: their properties end genesis. Soil Sci. Soc. Am. Proc. 17, 287–293.
Whitney, B.S., Mayle, F.E., Surangi, W.P., Fitzpatrick, K.A., Burn, M.J., Guillen, R., Chavez, E., Mann, D., Pennington, R.T., Metcalfe, S.E., 2011. Palaeogeogr. Palaeoclimatol. Palaeoecol. 307, 177–192.
Whittig, L.D., 1959. Characteristics and genesis of a Solodized Solonetz of California. Soil Sci. Soc. Am. Proc. 23, 469–473.
Wilding, L.P., Odell, R.T., Fehrenbacher, J.B., Beavers, A.H., 1963. Source and distribution of sodium in solonetzic soils in Illinois. Soil Science Society Proceedings 27, 432–438.
Zaidel'man, F.R., Ustinov, M.T., Pakhomova, E.Y., 2010. Solods of the Baraba Lowland and the Priobskoe Plateau: their properties and genesis and the methods of their diagnostics. Eurasian Soil Science 43, 1069–1082.
Zaidel'man, F.R., Nikiforova, A.S., Stepantsova, L.V., Krasina, T.V., Krasin, V.N., 2014. Concretions in typical chernozem, gleyed chernozem-like, and solonetzic chernozem-like soils of the outhern Tambov Lowland. Eurasian Soil Science 47, 540–555.
Zani, H., Assine, M.L., Araújo, B.C., Merino, E.R., Silva, A., Fancicani, E.M., 2006. Lobos deposicionais na evolução do megaleque do rio Taquari, Pantanal mato-Grossense. Anais do 1° Simpósio de Geotecnologias no Pantanal, Campo Grande, Brasil, 11-15/11/2006, pp. 285–292.
Zani, H., Assine, M.L., Silva, A., Corradini, F.A., 2009. Redes de drenagem distributária e formas posicionais no megaleque do Taquari¨, Pantanal: uma análise baseada no MDE-SRTM. Revista Brasileira de Geomorfologia 10, 21–28.